ADVANCED MATERIALS
www.advmat.de

# Modeling Single-Atom Catalysis

*Giovanni Di Liberto and Gianfranco Pacchioni**

**Electronic structure calculations represent an essential complement of experiments to characterize single-atom catalysts (SACs), consisting of isolated metal atoms stabilized on a support, but also to predict new catalysts. However, simulating SACs with quantum chemistry approaches is not as simple as often assumed. In this work, the essential factors that characterize a reliable simulation of SACs activity are examined. The *Perspective* focuses on the importance of precise atomistic characterization of the active site, since even small changes in the metal atom's surroundings can result in large changes in reactivity. The dynamical behavior and stability of SACs under working conditions, as well as the importance of adopting appropriate methods to solve the Schrödinger equation for a quantitative evaluation of reaction energies are addressed. The *Perspective* also focuses on the relevance of the model adopted. For electrocatalysis this must include the effects of the solvent, the presence of electrolytes, the pH, and the external potential. Finally, it is discussed how the similarities between SACs and coordination compounds may result in reaction intermediates that usually are not observed on metal electrodes. When these aspects are not adequately considered, the predictive power of electronic structure calculations is quite limited.**

## 1. Introduction

The search for new materials to be used in catalytic processes has a long history, and became an activity of industrial importance in the early 20th century. An important breakthrough was the discovery in 1913 of iron oxide as a catalyst for the synthesis of ammonia by Haber and Le Rossignol.[1] Since then, there has been a continuous search for new materials for advanced catalytic processes which continues to the present days. The vast majority of industrial plants and of environmental processes makes use of heterogeneous catalysts where reactants and products are in gaseous or liquid phase, while the catalyst is solid, thus allowing the latter to be separated from the products at the end of the reaction. Heterogeneous catalysts often consist of small aggregates of noble metals stabilized on a support (typically a bulk oxide or porous material such as a zeolite).[2,3] They are usually prepared by dispersion of a precursor, e.g., a salt containing metal ions, on the support followed by a treatment in hydrogen which leads to the formation of metal atoms which can diffuse and aggregate to form metal particles if the temperature is increased. The result is a broad distribution of metallic particles of different sizes and shapes, with a certain dimensionality dominating the ensemble. For a long time the presence of smaller entities such as nanoclusters or even isolated atoms was not considered in the discussion of their properties, mainly due to the fact that the available characterization methods were not able to identify these tiny minority species.[4]

Today, thanks to spectacular advances in spectroscopies and microscopies, it is possible to identify and characterize, at least to a certain extent, ultrasmall entities present on the surface of the catalyst support and reveal their catalytic role.[5] By designing specific preparation methods, it is also possible to obtain catalysts in which nanoaggregates, smaller than 1 nm, or even isolated atoms represent the dominant species. A new branch of heterogeneous catalysis, nanocatalysis, has emerged with the specific aim of dealing with catalysts based on very low amounts of precious metals dispersed over a surface.[6]

The ultimate limit of this approach is obviously a catalyst consisting of single-atomic species stabilized on a support. Stability is an essential aspect as the formation of metal–metal bonds is thermodynamically favorable, and if the atoms are allowed to migrate and diffuse on the support surface they will aggregate leading to the nucleation and growth of the metal particles. This sintering process is generally a detrimental aspect in heterogeneous catalysis as it reduces the surface area of the metal phase, with severe loss of activity. On the other hand, the chemical activity of an isolated atom or a metal cluster can be completely different from that of a metal particle containing hundred thousands or millions of atoms.[7] One interesting aspect of single-atom catalysts (SACs) is that they are often in positive oxidation state, a condition that should prevent the formation of metal–metal bonds and make nucleation and growth of nanoparticles less likely. Specific experimental and theoretical studies conducted in the last two decades of the last century have contributed to highlighting the strong changes in the chemical properties of small aggregates when the size (and shape!) is modified even slightly. The simple

G. Di Liberto, G. Pacchioni
Dipartimento di Scienza dei Materiali
Università degli studi di Milano Bicocca
Via R. Cozzi 55, 20125 Milano, Italy
E-mail: gianfranco.pacchioni@unimib.it

The ORCID identification number(s) for the author(s) of this article can be found under https://doi.org/10.1002/adma.202307150



**DOI: 10.1002/adma.202307150**

addition or removal of an atom to a cluster can result in complete changes in responsiveness. This is the nonscalable size regime typical of cluster properties.[8] It has advantages and disadvantages: on the one hand it makes possible, at least in principle, to regulate the activity by selecting the appropriate cluster size; on the other hand, the practical difficulty of generating monodisperse collections of clusters all having the same size inevitably leads to a variety of reaction paths, with negative consequences on the selectivity of the process. From this point of view, the possibility of working with isolated atoms bonded and stabilized on an inert support opens up new and interesting perspectives: one can work with easily separable solid systems, use a minimum quantity of metal catalysts and expect greater selectivity for a given reaction.

Some of these advantages are typical of homogeneous catalysts, i.e., catalysts that work in the same phase as the reactants and products. Typical examples are metal complexes in solution and enzymes. Due to their molecular nature, homogeneous catalysts are easier to characterize and their activity can be tuned by playing with the ligands bound to the active metal center. Unfortunately, many homogeneous catalysts suffer from thermal stability problems, unlike heterogeneous catalysts, which can sustain high reaction temperatures and pressures. Therefore, the idea of preparing catalysts based on single site active species that all have the same environment is very attractive and has been studied extensively in the past. For example, in the 1960s Arlman and Cossee identified under-coordinated Ti ions near Cl vacancies as the active sites in the $\alpha$-$TiCl_3$-based Ziegler–Natta catalyst.[9] A few years later one witnessed the birth of a still lively catalysis sector, known as surface organometallic chemistry.[10] Here the catalytic sites are formed by reacting an organometallic complex or coordination compound with a functionalized surface, usually an oxide with a high concentration of OH groups. The M–OH or M–O–M surface species react with one of the ligands of the coordination compound TM–$L_n$ (TM = transition metal, L = ligand), which is then anchored to the surface via M—O—TM—$L_{n-1}$ bonds. The supported organometallic compound retains at least a portion of the ligands that were originally present and is bonded via strong covalent bonds to the surface which acts as a super bulky ligand. The fields of surface organometallic and coordination chemistry have been reviewed extensively also recently.[11–14]

Past examples of single-site catalysts are numerous. In 1999 Iwasawa and co-workers demonstrated that isolated Pt atoms deposited on MgO and prepared by impregnation showed the same activity as Pt nanoparticles in promoting propane combustion.[15] In 2000, some of us reported a model study where mass-selected Pd clusters, including Pd atoms, were deposited on a MgO(100) surface and studied their capability to catalyze the trimerization reaction of acetylene to benzene.[16] Surprisingly, isolated Pd atoms were found to be good catalysts for the reaction, provided they were located on specific defect sites, the oxygen vacancies present on the MgO surface. The novelty of this result was clear from the title: "Acetylene cyclotrimerization on supported size-selected $Pd_n$ clusters: One atom is enough!". The work also contained another relevant concept in this field: the support plays a key role in determining the properties of the metal atom.

An important step in this field was the discovery in 2003 by Flytzani-Stephanopoulos and co-workers that Au or Pd atoms supported on ceria, $CeO_2$, are active in the water-gas-shift reaction.[17] A few years later Gates reported a nice example of a fully characterized Ir complex stabilized on two different matrices, a zeolite and the MgO surface. Catalytic tests were performed and it was found that the rates of catalytic ethene hydrogenation and $H_2/D_2$ exchange were more than an order of magnitude higher on the zeolite than on the MgO support, highlighting the role of the environment in the chemistry of the supported Ir atom.[18] A few years later Gates and co-workers were able to fully identify the MgO surface sites where Ir is stabilized, showing that each Ir atom is bound to three O atoms of the MgO surface.[19]

A dramatic change in the field occurred in 2011 when Zhang and co-workers reported the preparation, characterization and catalytic testing of a $Pt_1/FeO_x$ catalyst consisting of single Pt atoms supported on iron oxide.[20] The presence of individual Pt atoms was clearly demonstrated and, more importantly, the term "single-atom catalysis" (SAC) was coined for the first time. The possibility of identifying individual atoms and studying their activity in a variety of reactions has stimulated a rapid growth of works devoted to this topic. Various supports have been tested in addition to the classic oxide surfaces commonly used to deposit metal nanoparticles: carbon-based materials, metal–organic frameworks (MOFs), covalent organic frameworks (COFs), 2D materials (variously doped graphene, sulphides, MXenes, etc.).[21–27] Recently the concept of a single-atom nanozyme has been formulated, where the goal is to reproduce the intrinsic activity of enzymes by tuning the spatial configuration of the active single-atom site.[28,29]

The number of reactions in which SACs are involved has also grown rapidly, passing from the more classic CO oxidation to hydrogenation reactions, water splitting, ammonia synthesis, $CO_2$ reduction, organic synthesis, etc.[22,30,31] In addition to thermal catalysis, SACs are also intensively studied in electrocatalysis and photocatalysis.[32,33]

The name "single-atom catalyst", today commonly used to indicate solid catalysts in which the active site consists of a TM atom stabilized in a matrix, is certainly attractive and suggests that isolated metal atoms are the key catalytic species. The idea of having a single atom incorporated in a lattice which is responsible for changes in surface reactivity is interesting and reminiscent of the more classic notion of dopants or impurities in materials science. When heteroatoms are embedded on the surface of a solid, e.g., an oxide, they modify the chemical properties through various mechanisms, which are linked to the specific orbitals of the dopant and their occupation.[34] Dopants can occupy substitutional or interstitial positions on the upper layers of a solid surface. There is an abundant literature on the chemistry of doped oxide surfaces.[35] In many cases the notion of doped surface and that of SAC coincide, despite the very different way of naming them.

## 2. Role of the Metal and of Role the Support

The term SAC suggests that the properties of the active site are intimately connected with those of the supported atom. This is only partially true, and in fact we have already mentioned cases in which the interaction with the support has been clearly highlighted.[16] The fact that the atoms surrounding the central metal atom play important roles not only on the catalytic

activity but also on the selectivity and stability has been recently emphasized.[36] Tang et al. have shown that a control on the first and second coordination spheres of a Co-based SAC determines the electrocatalytic response in acidic oxygen reduction reaction (ORR). In particular, the ORR selectivity can be tailored from a four-electron to a two-electron pathway by modifying the first (N or/and O) and second coordination spheres (functionalization of the carbon substrate). The change in selectivity originates from the shift of the active sites from the center Co atom to the O-adjacent C atom.[37] Sometimes even the symmetry of the active site is important: Cho et al. have shown the key role of three-coordinated $Pt^{II}$ SACs with broken $D_{4h}$ symmetry in electrocatalytic chlorine evolution reaction.[38] Possible strategies to manipulate in a desired way the coordination environments of SACs have been suggested based on: a) the selection of the metal atom, b) the modification of the local environment to the metal center metal, and c) the modification of the geometric configuration of the support.[39]

To further show how the local coordination around a SAC can determine the overall reactivity let us consider a simple computational experiment based on the density functional theory (DFT).[40] A set of 24 TM atoms has been stabilized on a nitrogen-doped graphene support (4N-Gr) and their reactivity has been tested in the hydrogen evolution reaction (HER). The adsorption free energy of a H atom adsorbed on the SAC, $\Delta G_H$, is considered a good proxy of the overall reactivity, according to the computational hydrogen electrode (CHE) model proposed by Nørskov and co-workers.[41] In particular, a $\Delta G_H$ close to zero is indicative of a good catalyst (low overpotential) while conditions where $\Delta G_H$ is large in absolute value indicate a poor catalyst or even a totally inactive material.

By changing the TM atom in the TM@4N-Gr matrix one obtains a range of $\Delta G_H$ values that go from +2.17 eV (Au, inert), to −1.14 eV (Hf, inert) with Co exhibiting the highest activity, $\Delta G_H = 0.1$ eV. However, if one fixes the metal atom, e.g., Pt, and replaces with C or O the N atoms first neighbors to the TM one can generate about 20 structures that differ only for the local coordination (N, C, and O first neighbors). In this way the hydrogen adsorption free energy on the Pt atom, $\Delta G_H$, goes from +1.54 eV (4 N atoms bound to Pt) to −1.60 eV (1 N and 3 O atoms bound to Pt). This is more or less the same range of $\Delta G_H$ values, about 3 eV, obtained by keeping the matrix fixed and changing the TM atom.[40] Stated differently, the reactivity of a SAC can be tuned in the very same way by changing the TM atom or by keeping the TM atom fixed and varying the neighboring atoms of the support. At least in principle. One should not forget that one of the main issues with the preparation of catalysts based on single atoms is their stability, and that very stable SACs are usually less reactive, while high reactivity is predicted for less stable species. The interplay between coordination, activity, and stability is central in the design of new systems.

## 3. Importance of Structural Characterization

This opens an essential item for the development of new active SACs: the precise identification and characterization of the active site. Since the local coordination is so important in determining the reactivity, the rational design of new SACs based on computational screening requires a control at atomistic level of the structure of the experimental catalyst. While this is rather standard in homogeneous catalysis where the active species is a TM atom surrounded by a well-defined ligand shell, it is quite difficult and challenging when one moves to solid materials and surfaces. Notice that here we refer only to the local environment of a SAC in the as-prepared catalyst, i.e., before the reaction takes place. In fact, under working conditions, new species and intermediates can form and coordinate to the metal center, altering the properties of the active site. This aspect, specifically related to the formation of uncommon reaction intermediates, will be discussed below in the context of the modeling of the reactivity of SACs.

A variety of techniques and approaches have been developed or used over the years to better identify the nature of SACs: X-ray photoemission spectroscopy (XPS) and X-ray adsorption spectroscopy provide info on the oxidation state of the metal, extended X-ray absorption fine structure (EXAFS) spectroscopy is essential to gain info on the local coordination of the TM atom, of the bond distances, and to exclude the presence of metal–metal bonds that occur when metal particles are present. Diffuse reflectance spectroscopy in UV or visible light (DRUV–vis) helps to distinguish isolated sites from aggregates. Solid-state NMR can also be used to characterize the nature of the catalyst and the dynamics of surface sites. Of course, aberration corrected scanning transmission electron microscopy coupled to high-angle annular dark-field detection remains an essential component of the characterization of every SAC. Several excellent reviews can be found on this topic.[32,42,43]

In this respect, particularly relevant and useful are studies performed on model systems with advanced characterization methods that allow an atomistic resolution of the species present on a surface. This is the case of scanning tunneling microscopy (STM) and spectroscopy studies combined with DFT simulations on precisely defined single-crystalline supports prepared in ultrahigh-vacuum. In this way it has been possible to follow, in particular, nature and evolution of SACs on the surfaces of rutile and anatase $TiO_2$, the iron oxides $Fe_2O_3$ and $Fe_3O_4$, as well as MgO films and $CeO_2$.[44,45]

Recently we have shown that the combination of Fourier transform infrared spectroscopy and thermal desorption spectroscopy of adsorbed probe molecules with DFT calculations can be extremely powerful to identify the bonding environment of a metal atom.[46–51] CO is widely used to probe the nature of a surface site thanks to its high sensitivity and low reactivity. The combined measurement of CO vibrational properties and adsorption energy, and the comparison of these quantities with DFT calculations provides a powerful way to unambiguously identify the nature of the active sites on a solid surface.

The structure of Rh, Ru, and Pt SACs stabilized on anatase $TiO_2$ or tetragonal $ZrO_2$ has been elucidated in this way.[46–50] The strategy consists in performing a series of DFT calculations where the TM atom is placed in all possible positions on the oxide surface: the TM can replace a surface cation, $TM_{subCat}$, or a lattice O anion, $TM_{subO}$; it can be adsorbed on various sites of the surface, $TM_{ads}$, or it can form $TM(O)_{ads}$ or $TM(O_2)_{ads}$ adsorbed units, where the TM is anchored to the surface via extra O adatoms. Finally, it can bind to hydroxyl groups, usually present on oxide surfaces, forming $TM(OH)_{ads}$ species. Each of these sites can then be structurally optimized at the DFT level, and CO can be adsorbed on the TM atom. The corresponding bonding and

vibrational properties of the resulting TM(CO), $TM(CO)_2$ or $TM(CO)_3$ surface complexes can be computed from first principles, generating a library of characteristic features of the site. These data can be combined with the experimental observations. The IR and TPD spectra of adsorbed CO can be collected as a function of increasing temperature, causing the selective desorption of CO, thus providing changes in the vibrational spectra and of the TM—CO bond strength (e.g., while symmetric and antisymmetric CO stretching are present for $TM(CO)_2$, only one band is present in TM(CO)).

The systematic study of Rh, Ru, or Pt SACs on $TiO_2$ and $ZrO_2$ showed that the TM atom is stabilized by the interaction with one or two O atoms or OH groups on the oxide surface. In these sites, $TM(O)_{ads}$, $TM(O_2)_{ads}$, $TM(OH)_{ads}$, the TM atom is formally in a positive oxidation state, a result that agrees also with XPS data, and is thermally stable thanks to the anchoring role of the extra O atoms or OH groups.[52] Strong evidence for the assignment comes from the excellent agreement between theory and experiment in CO adsorption energies and vibrational frequencies. It is important to mention that the agreement of just one of these properties is not enough to safely conclude about the nature of the SAC, while the combination of more than one measured and computed property provides a robust indication that this is the actual species present on the surface.

However, the calculation of the CO stretching frequency is not without problems. For instance, the identification of the sites where Au atoms are bound on the (001) surface of $LaFeO_3$ turned out to be a complex case. A comparison of standard and hybrid DFT functionals with high-level quantum chemistry methods has shown the difficulty of advanced DFT approaches to reproduce quantitatively the large blue shifts of the C—O vibrational frequency observed in the experiments, a problem that emerges when the CO molecule is bound to $Au^{\delta+}$ atoms in a positive oxidation state.[51]

Despite spectacular progress in identifying isolated atoms trapped on a given solid material, the exact nature of the local bonding still remains elusive. This is a problem when computational studies are used to complement experimental evidence of SACs activity. Indeed, only if the nature of the active site is known with sufficient accuracy and reliability, a comparison between calculated and measured properties is meaningful (not to talk of predictions of new catalysts). In this regard, even a cursory analysis of the literature on the subject reveals that in most cases the exact nature of the active site of a SAC is simply guessed but not proven beyond any doubt. Even when it is assumed that a SAC corresponds to a given structural model, the evidence from the characterization methods used is often only partial.

## 4. SACs as Dynamic Species

Another problem related to the structural characterization of SACs is their potential dynamical behavior under reaction conditions. A pioneer in homogeneous catalysts, Jack Halpern, once said that "if you can identify a compound from a catalytic system, it is probably not the catalyst".[53] Indeed, it is well known that the active site of a catalyst may form in the course of the reaction and can change as a function of the external conditions of temperature and pressure. For this reason, operando spectroscopies

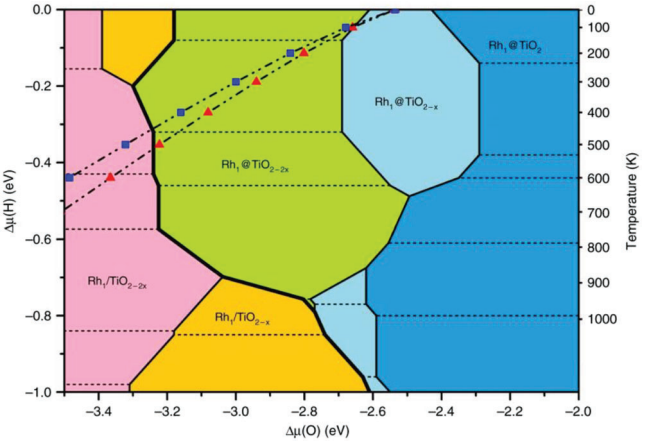


**Figure 1.** Surface stability diagram for a Rh atom on $TiO_2$(110). $\Delta\mu$(H) and $\Delta\mu$(O) indicate the H and O chemical potentials. Different colors indicate the various configurations for the Rh and the $TiO_2$ surface: blue, light blue, and green denote regions where Rh is preferentially substituting a six-coordinated surface Ti with zero, one, or two O vacancies ($Rh_1@TiO_2$, $Rh_1@TiO_{2-x}$, $Rh_1@TiO_{2-2x}$) and orange and pink zones where the supported Rh structure is favored ($Rh_1/TiO_{2-x}$ and $Rh_1/TiO_{2-2x}$), respectively. The amount of hydrogen adsorbed on $TiO_2$ and Rh depends on $\Delta\mu$(H) and dashed lines limit the zones corresponding to different hydrogen coverage. The red triangle (blue square) line shows the relation between $\Delta\mu$(O) and $\Delta\mu$(H) when water formation reaction is included with 0.01% (0.001%) conversion. $\Delta\mu$(H) values for 0.1 atm $H_2$ and various temperatures are shown on the right vertical axis. Reproduced under the terms of the CC BY Creative Commons Attribution 4.0 International license (https://creativecommons.org/licenses/by/4.0).[55] Copyright 2019, The Authors, published by Springer Nature.

have been developed with the specific aim to follow the temporal evolution of a catalyst under reaction conditions.[54] Of course, this applies also to SACs, although the number of cases reported with a detailed characterization of the structural evolution of a SAC with time are still rare.

Theory is useful in this respect as it can provide phase diagrams that show under which conditions a given structural motif is stable. An example has been reported for the case of $Rh_1/TiO_2$ based on first principles atomistic thermodynamics.[55] Using two descriptors, the oxygen and hydrogen chemical potentials, the relative stability of a Rh atom adsorbed or in substitutional positions of rutile $TiO_2$ has been evaluated as a function of temperature, clearly showing that the Rh single atoms modify their local coordination (and reactivity!) in response to various redox conditions, an effect that has been verified experimentally.[55] In particular, when the catalyst is treated in a reducing $H_2$ atmosphere $Rh(OH)_{ads}$ complexes form, as discussed above, while under strong oxidizing conditions the Rh atoms become preferentially incorporated in the oxide lattice, see **Figure 1**.

The dynamic nature of SACs has been demonstrated for the case of $Pt_1/TiO_2$ based on in situ atomic resolution microscopy and spectroscopy characterization complemented by first principles DFT calculations.[56] Under oxidizing conditions the Pt atoms are incorporated into the anatase $TiO_2$ lattice, and in particular replace $Ti_{5c}$ ions at the surface or near step edges; this is the same as predicted for Rh, see Figure 1, since in oxidizing conditions the TM prefers to be part of the support. However,

in mild reducing conditions the substitutional Pt atoms are pulled out of the surface, and become bound to extra surface O atoms coming from surface OH groups, forming $Pt(O_2)_{ads}$ species. If the catalysts is further treated in $H_2$ at higher temperature (harsh reduction), one observes the formation of $Pt(OH)_{ads}$ species adsorbed at steps and terrace sites. Thus, the nature of the SAC changes significantly with the pretreatment of the catalyst, with considerable impact on the reactivity.[56] To check this, CO oxidation was studied on the Pt SACs as a function of the catalyst pretreatment finding that when Pt occupies substitutional sites, $Pt_{subCat}$, or is bound to excess O atoms, $Pt(O_2)_{ads}$, the reaction proceeds with similar apparent activation energies, $E_a$, of 70–80 kJ mol$^{-1}$. However, after harsh reduction, the $Pt(OH)_{ads}$ species showed a twofold to fivefold increase in activity, depending on temperature, and a decrease in $E_a$ to 48 kJ mol$^{-1}$. Thus, the activity of the Pt SAC is markedly different for the three sites structurally characterized. The Pt atomic species on titania can adopt a range of local coordination environments in response to changes in the conditions, a phenomenon that is reminiscent of the dynamic behavior of metal ions in zeolites.[57]

Of course, under particular conditions of temperature and pressure, also the structure of the support itself can change and give rise to new structures and compositions. Several examples have been reported, in particular for oxide surfaces, after the seminal work of Reuter and Scheffler who introduced the idea of ab initio thermodynamic analysis for the study of the evolution of the $RuO_2$ surface as a function of the external conditions.[58]

In the field of carbon-based support, an example of structural evolution of a SAC is that reported by Yang et al.[59] who fabricated Cu–N–C SACs with a well-defined $Cu^{2+}$–$N_4$ structure. By combining operando X-ray absorption spectroscopy with DFT calculations, the authors showed the dynamic evolution of Cu–$N_4$ to Cu–$N_3$ and further to HO–Cu–$N_2$ under ORR working conditions, and the simultaneous reduction of $Cu^{2+}$ to $Cu^+$. Notice that the low-coordinated $Cu^+$–$N_3$ species that forms in the course of the reaction is the real active site.

In general, dealing with the fluxional nature of SACs (and small nanoparticles in general) is extremely important. Particularly challenging is to distinguish thermodynamic and kinetic stability. Computationally, the thermodynamic stability can be addressed relatively easily provided that all relevant deactivation routes are considered. On the contrary, accessing the corresponding kinetics is very challenging for processes such as dissolution (under oxidative conditions) or nanoparticle formation (under reducing conditions). A nice approach to these problems has been proposed recently by Poths and Alexandrova.[60] This is based on the utilization of specific computational techniques and approaches to enable atomistic characterization of the most relevant catalytic sites under operating conditions.

This brief and incomplete list clearly shows two things that should always be kept in mind in the discussion of the reactivity of SACs and the corresponding modeling: 1) the support matters a lot, and any structural detail or change in the local environment can have dramatic effects on the reactivity; and 2) even if the structure of the SAC has been identified with atomistic precision, one should make sure that the atom stays put during the reaction as SACs can behave as dynamical species, making their identification more complex.

## 5. First Principles Calculations of SACs: How Accurate Are They?

The 1998 Nobel Prize in Chemistry went to John Pople, "for his development of computational methods in quantum chemistry", and Walter Kohn "for his development of the density functional theory".[61] This is considered the moment when quantum chemistry has become a mature field and a fundamental support to the experiment. Since then, there have been spectacular advances in modeling complex systems in diverse areas, from medicinal chemistry, biochemistry, organic synthesis and, of course, catalysis. Unsurprisingly, electronic structure calculations have also been used to unravel the nature of the new class of catalytic materials known as SACs.[62] In recent years we have witnessed an explosion of calculations performed at various levels to rationalize observation but above all to predict new active catalysts.[63,64] The feeling is that, compared to other more traditional areas of catalysis, the field of SACs has attracted uncommon attention from the computational chemistry community.

There are various reasons for this interest. One is the fascinating nature of SACs, where important catalytic reactions can be performed thanks to a single active center. Other reasons are related to a classic problem in computational modeling: the complexity of the system to be simulated.[65] In heterogeneous catalysts the catalyst consists of a metal particle stabilized on the surface of an "inert" support, usually an oxide. This already implies to consider the nature of the metal/oxide interface, a region which is difficult to access experimentally and which remains structurally and electronically less defined. The catalytic reaction can occur on the various facets of the metal particle, on low-coordination metal sites at steps or edges, or even at the metal/oxide interface, a region where the chemical behavior can be very different from that of the individual components.[66] Oxide surfaces are rich in morphological and point defects, can be partially or totally hydroxylated, and exhibit a dynamic behavior which depends on the external conditions of temperature and pressure.[67] This is even more true for the metal particle, particularly when the size is small. Here the reactivity can critically depend on several factors, first of all the size. Metallic clusters can adopt a variety of shapes, resulting in a myriad of potential structural motifs, often experimentally unknown. Finally, diffusion of interstitials from the bulk to the surface or of adsorbates in the bulk is another phenomenon that can occur. This incomplete list of phenomena that contribute to the final catalytic activity shows how difficult it is to build realistic models that mimic the actual active phase of a heterogeneous catalyst.

From this point of view, SACs are apparently simpler systems. The active phase consists of a single metal atom, eliminating the problem of dealing with large distributions of particle sizes and shapes; the support matrix is often made up of light materials considered less defective than the oxide surfaces (e.g., graphene, carbon nitride, etc.); for 2D supports, the system to be modeled is much smaller than that of a classical heterogeneous catalyst: instead of supercells containing multiple oxide layers and dozens of metal atoms, one is dealing with single layers of main group elements such as carbon. As we will show later, the greater simplicity of SACs compared to the classic supported metal particles is more apparent than real. In fact, modeling SACs and their activity presents a greater complexity than often assumed and

poses several problems for theorists in order to build realistic models.

The other aspect of the chemistry of SACs that has received less attention than it deserves is the accuracy of the computational method used. It is well known that the exact solution of the Schrödinger equation is possible only for extremely small systems, while here we are dealing with hundreds of atoms. This requires approximations in the methodology adopted and results in error bars in the quantities calculated. While obvious, there is a tendency to forget this aspect and put an absolute value on the calculated reaction energies, one of the quantities of central interest in quantum chemistry. This is especially true for DFT calculations, whose results are strongly dependent on the expression of the exchange-correlation (xc) functional adopted.[68]

Different formulations of xc functionals have been proposed in the literature; they give sometimes slightly different and sometimes quite different estimates of reaction energies. Without going into details, a broad distinction can be made between semilocal generalized gradient approximation (GGA) functionals that are uncorrected for the self-interaction error and functionals that are partly corrected for self-interaction. To the first category belong the widely used PBE functional[69] and others (PW91,[70] BLYP[71,72]); the second group includes the so-called hybrid functionals (B3LYP,[73,74] PBE0,[75,76] HSE06[77] are the most common) and the DFT+$U$ functionals (e.g., PBE+$U$[78]). It goes without saying that the functionals partly corrected for self-interaction are superior and provide more robust descriptions of the band structure of semiconductors and insulators, electron localization, and even thermochemistry.[79] In this context, the DFT+$U$ approach represents a pragmatic view to address the problem, as it is computationally less demanding than the use of hybrid functionals. However, it suffers from the fact that the results may depend critically on the choice of the U parameter. Despite this well-known dependence of DFT results on the choice of the functional, this aspect is very rarely discussed when it comes to calculating and predicting properties of SAC: the vast majority of the reported calculations are based on standard functionals, in particular the PBE one. It is important to mention in this context that nowadays post-HF methods (which are self-interaction free) are slowly coming into the realm of catalysis, for instance in the form of embedded multireference methods.[80,81]

In the study of molecular systems with quantum chemical methods it is common practice to benchmark the results of any approximate approach against highly accurate, and computationally intensive, wave function-based solutions of the Schrödinger equation, such as multiconfiguration methods or the coupled-cluster (CCSD(T)) approach.[82,83] While this can be done for relatively small molecular systems, it becomes hardly accessible for large molecules and periodic crystalline solids. However, in some cases SACs possess bonding environments that are reminiscent of those of inorganic complexes, opening the possibility to compute at various levels of theory the catalytic performance of a given molecular model of SAC.

Patel et al.[84] studied the reactivity of a Cu/2-phen system in the oxygen reduction reaction (ORR) at the CCSD(T) level of theory. The Cu/2-phen complex presents a bonding environment that is similar to that found in various SACs stabilized on carbon matrices. Overall, the binding energies of various intermediates predicted by PBE0 and HSE06 hybrid functionals were found to be in close agreement with the CCSD(T) ones with a mean absolute error (MAE) of 0.1 eV. The hybrid functionals describe the electronic structure and the bonding properties of this system more accurately than the GGA functionals ($MAE_{GGA}$ = 0.6–0.7 eV), thus highlighting the large errors associated to this approach. In their paper the authors concluded that "the results suggest that the blind use of GGA functionals to describe single-atom catalysts may produce inaccurate results".[84] This message, while relevant, is largely neglected in the computational modeling of SACs.

A further proof comes from a recent study dealing with the activity in the HER and oxygen evolution reaction (OER) reactions of 16 SACs consisting of TM atoms embedded in nitrogen-doped graphene (4N-Gr).[85] This work highlighted the importance of comparing different functionals when searching new potential catalysts from DFT calculations. Taking the HER as a reference, the GGA–PBE functional appears acceptable for 4d and 5d metals. Here the difference in reaction energies between PBE (standard GGA) and PBE0 (hybrid functional) is <0.2 eV, with some notable exceptions, such as Pt@4N-Gr where the difference is of 0.44 eV. However, for systems containing 3d TM atoms the use of PBE instead of PBE+$U$ or even better PBE0 functionals results in errors of 0.5 eV or more, with dramatic consequences on the prediction of the catalytic activity, **Figure 2**. For example, Co@4N-Gr is predicted to have $\Delta G_H$ = 0.13 eV at the PBE level, but this becomes 0.57 or 0.60 eV at PBE0 and PBE+$U$ levels of theory, respectively. This is the difference between an active catalyst (PBE) and an inert catalyst (PBE0 or PBE+$U$). Thus, the effect is not only quantitative, but also qualitative.

The difference between 3d and 4d–5d TM elements is easily explained by the fact that 3d TM atoms embedded in a solid matrix often assume magnetic ground states, in contrast to 4d and 5d TM atoms which give rise to closed shell systems. The magnetic moment of a SAC is a quantity that critically depends on the adopted computational method, an aspect that is often neglected in the discussion of the problem.

While the choice of the functional is probably the most delicate aspect, there are many other details of electronic structure calculations that can affect the final accuracy of the results: the dimensions of the supercells used (hence the coverage of the adsorbates or the density of active sites), the convergence criteria, the inclusion of dispersion at various levels of theory, the cut-off of plane wave basis sets, etc. We recently showed that while these effects are small in general, they introduce an error bar of at least 0.1 eV on the final calculated reaction energies.[86]

It emerges from the above discussion that several factors contribute to the final accuracy of an electronic structure calculation, particularly when reaction energies are involved. What can be considered small and therefore acceptable uncertainties, oscillations of ±0.2 eV in thermodynamic quantities or in reaction barriers, can significantly influence the prediction of an active SAC. This aspect adds to other problems that should be considered when using quantum chemistry methods to study catalytic reactions, related to the stability of the active phases, the interaction with the solvent when the reaction involves a solid/liquid interface, the formation of unusual intermediates or chemical species that can block the active site, etc. In the following sections we will address some of these aspects, demonstrating that the

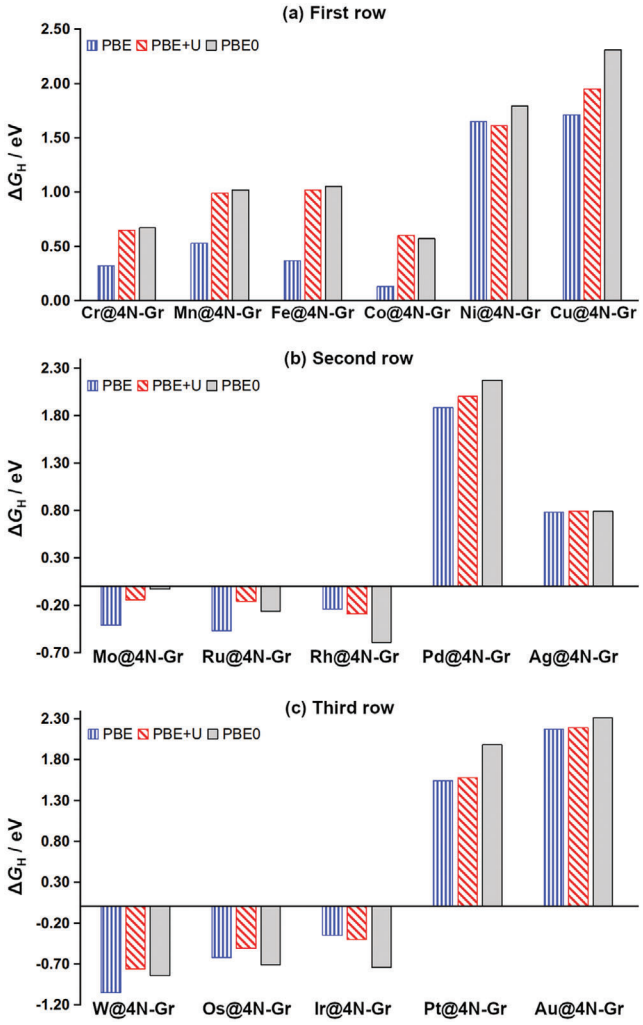


**Figure 2.** Gibbs free energy of hydrogen adsorption, $\Delta G_H$, for TM@4N-Gr SACs at PBE, PBE+$U$ and PBE0 levels of theory. Reproduced with permission.[85] Copyright 2022, The Authors, published by Wiley-VCH.

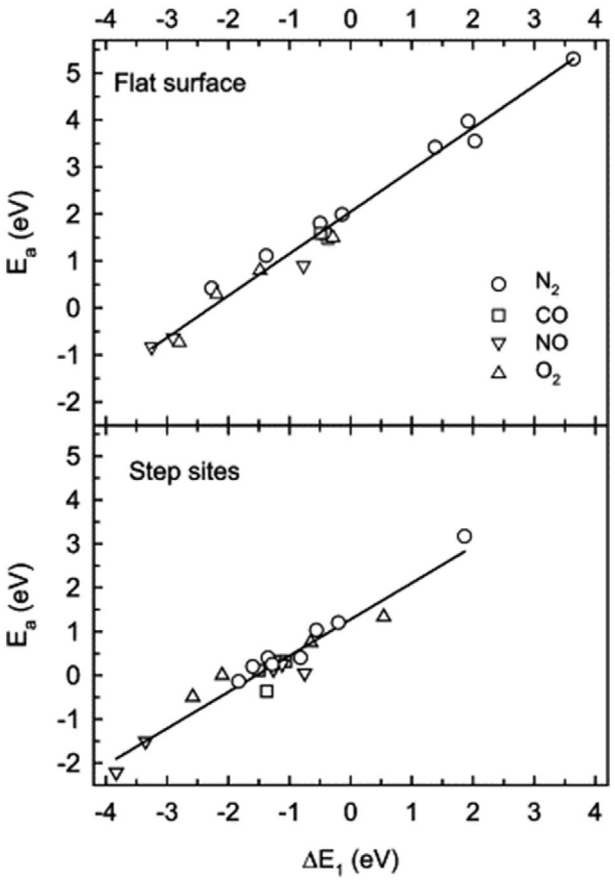


**Figure 3.** Calculated transition state energies ($E_a$) vs dissociative chemisorption energies ($\Delta E_1$) for $N_2$, CO, NO, and $O_2$ on a number of transition metal surfaces. Results for close packed as well as stepped surfaces are shown. Reproduced with permission.[89] Copyright 2004, Elsevier.

complexity inherent in modeling SACs is no less than that of more conventional supported metal particles.

## 6. Modeling Reactivity of SACs

### 6.1. Thermodynamic Approach

When modeling a catalytic process, the thermodynamic stability of the reactants and products must be taken into account, thus passing from the calculated energy differences ($\Delta E$) to Gibbs free energies ($\Delta G$). This implies to add to the calculated DFT energies ($\Delta E$) the entropic contribution ($\Delta S$) that can be taken either from international tables or determined ab initio using the formalism of the partition function. In addition, one must consider that reaction energies should be corrected by the zero-point energy contribution ($\Delta E_{ZPE}$), which is often very important for systems containing hydrogen atoms.[87,88] Chemical processes typically occur following activated pathways, and this involves modeling transition states and reaction barriers. Therefore, thermodynamic stability and reaction barriers are key ingredients. In many cases it is possible to simplify this picture thanks to the direct correlation between the binding energy of the reaction adsorbates and the corresponding activation energy. This correlation typically follows the linear Bronsted–Evans–Polanyi relationship stating that the difference in activation energy between two reactions is proportional to the difference in their reaction enthalpy.

Norskov and co-workers proposed in 2002 the existence of a universal relationship between the adsorption energy of different adsorbates and the activation energy independent of reactants and catalysts,[89,90] see **Figure 3**. This relationship was identified a few years before by Pallassana and Neurock in a study of C—H bond activation on Pd surfaces.[91] In the work of Bligaard et al.[89] it was shown that the dissociative chemisorption energy for a number of diatomic molecules, i.e., the energy change associated to the rate-determining step, is usually a good descriptor of the catalytic activity of a given metal. If the activity is plotted as a function of this descriptor, one obtains a volcano curve. Thus, it is possible to extract relevant catalytic information on the reaction energy profiles by adopting an ab initio thermodynamic approach, i.e., neglecting reaction barriers other than those deriving from thermochemistry.[41] Later it was shown that these

scaling relationships can be broken, and, being material dependent, are not universal.

### 6.2. Kinetic Approach: Reaction Barriers and Microkinetic Approaches

Once the thermodynamic energy profile is obtained, the reliability of the model can be improved by including reaction barriers. Finding the reaction barriers is a complex problem, as it involves determining the saddle points along the potential energy surface. In chemistry, once the transition states have been determined, the lowest energy path that connects reactants and products passing through the transition states defines the reaction coordinate. An extremely powerful tool for determining transition states and reaction profiles is the nudged elastic band (NEB) approach.[92] The NEB is a method for finding minimum energy paths and identifying putative candidates for the transition state structures (saddle points between reactants and products) that need to be characterized by frequency analysis. It is based on the optimization of a number of intermediate images along the reaction path where each image corresponds to the lowest energy while maintaining an equal spacing to the neighboring images.

Alternative ways to map the potential energy surface are based on advanced free energy surface sampling techniques such as metadynamics.[93,94] Metadynamics is a technique that allows the estimation of the free energy of complex molecular systems and the acceleration of rare events. It is based on "filling" the potential energy by a sum of Gaussians centered along the trajectory followed by an appropriate set of collective variables, thus forcing the system to migrate from one minimum to the next.

The thermodynamic stability of reaction intermediates and transition states can be used to feed microkinetic models to calculate reaction rates, assuming specific reaction energy paths and reaction conditions such as quasi equilibrium or the steady-state approximation. Indeed, microkinetic modeling allows somewhat to connect atomistic information (stability of reaction intermediates and reaction barriers) with chemical observables such as reaction rates, or to provide comprehensive understanding of complex reactions such as oxygen evolution or water gas shift.[95,96] An alternative approach to account for kinetics is based on kinetic Monte Carlo. This method simulates the time evolution of chemical reactions. The information about energy minima and transition states is given as input to the algorithm, as the method itself cannot predict them. The methodology is quite expensive because it requires to sample the potential energy landscape through molecular dynamics trajectories that can be very long and heavy to compute. However, it represents a potential framework to bridge the nano- and microcatalytic scales.[97]

## 7. Modeling SACs under Working Conditions

### 7.1. Gas-Phase Environment

The ingredients discussed above can be used to model the catalytic reactions that occur at solid/gas interface. Entropic contributions of gas-phase species can be taken from the international tables, when available, or can be determined by calculation of the partition function including configurational, translational, and vibrational degrees of freedom. For adsorbed species entropy contributions can be computed from the vibrational frequencies needed to obtain the zero-point energy and to confirm the minimum character of the adsorbate on the potential energy surface. Nevertheless, a common approximation is to neglect the entropy of the solid-state species. The seminal work by Campbell and Sellers also proposed a working equation for determining the entropy of adsorbates from the standard entropy of their gas-phase counterparts.[98]

Finally, we underline that the reaction energies must be corrected for the zero-point energy, since even at 0 K the effective energy of each chemical system does not correspond to the minimum value along the potential energy profile. This is particularly relevant for systems involving hydrogen atoms.[99] Finally, the vibrational nature of systems is usually approximated in a harmonic fashion, which is often reasonable, but one should consider that in some cases anharmonicity plays a role.[100,101] In particular, a nice overview underlining the importance in activation energies appeared recently.[102]

### 7.2. Electrochemical Environment

Electrochemical processes take place in a solvent under certain working conditions of pH and applied voltage, and an electrolyte is present in solution. All these effects can play a role. Before discussing some relevant strategies for dealing with them, directly or indirectly, let us recall the already mentioned CHE model,[41,87] a popular framework when dealing with electrochemical processes. This was originally formulated in a seminal work by Anderson[103,104] who devised a conceptually equivalent (albeit with a different hypothesis on the transferability) approach. The method assumes that the reaction steps involve the simultaneous exchange of electrons and protons. This is very difficult to simulate, requiring modeling a charged electrode and to introduce explicitly a $H^+$ ion into the system. The basic idea of CHE is to consider that in standard conditions the following equation is verified

$$\Delta G_{H_2} = \Delta G_{H^+} + \Delta G_{e^-} = 0.00\,\text{eV} \quad (1)$$

Based on it one can replace the Gibbs free energies of $H^+ + e^-$ with that of a $H_2$ molecule, much simpler to calculate. Usually, in electrochemical reactions $H^+$ and $e^-$ work together; this allows to model not only the HER but many other reactions. In the following we briefly analyze the importance of each of the aspects that contribute to refine the computational model: solvation, electrolyte, pH, and voltage.

#### *7.2.1. Solvation*

Solvation has several effects, as the solvent can alter the stability of a catalyst leading to dissolution of ionic species, can change the arrangement of exposed atoms, affect the stability of reaction intermediates, and even open or block specific reaction channels.

The solvent can be treated in many different ways.[105] It can be implicitly included in the model by replacing the vacuum with a dielectric medium that mimics that of the solvent.[106] This approach is extremely popular and has proven to be very useful due to its practical application and relatively low computational cost. The solvent can also be treated explicitly by adding a large number of solvent molecules into the simulation box to generate a catalyst/solvent interface and to ensure a bulk-like behavior of the solvent as one moves away from the interface.[107] Guo et al.[107] also showed the importance of treating explicitly at an atomistic level the water–electrode interface.

The typical solvent for electrochemical processes is liquid water which is characterized by hydrogen bonds and by relatively important secondary interactions with a specific directionality. This often makes the treatment of explicit solvation essential when dealing with water.[108,109] Water is also very functional and dynamic effects are important. This implies the use of ab initio molecular dynamics (AIMD) simulations.[110–113] In a recent study the OER has been considered on the surface of a $RuO_2$ catalyst. Here a hydrogen bond with a surface OH group stabilizes an unconventional —OO intermediate (—OO—H), besides the classical —OOH one, before $O_2$ evolution takes place. AIMD is essential to show that both intermediates participate in a hydrogen bonding network with water but leading to different interfacial water structures; in particular, the —OOH species can spontaneously convert into —OO—H. This is a case where the adoption of static solvation approaches tends to overestimate the energetic difference between two reaction intermediates, with important effects on the dynamical structure of the water/oxide interface.[111]

AIMD calculations are computationally very intensive and a critical problem is represented by the propagation times needed to reach equilibration.[114] A possible solution to overcome this limitation is to adopt prefitted potential energy surfaces or force fields parameterized ad hoc. Alternatively, approximate schemes can be adopted.

We discuss here two examples, the water bilayer model and the microsolvation approach. In the first, solvation is approximated by modeling a static layer having a periodic, crystalline arrangement of water molecules. The main limitation is that the model is quite rigid and it is necessary to work with suitable supercells capable of accommodating the solvent without introducing spurious strain effects. However, the bilayer model allows solvation to be accounted for with acceptable computational costs. Recently this model has been applied to the study of $N_2$ reduction reaction on SACs supported by thiophene-linked porphyrin.[115] In order to treat solvation with moderate computational cost the microsolvation approach has been proposed.[116–118] It was shown that just three water molecules are sufficient to capture the main contribution of coadsorbed water to the adsorption energies of OH* and OOH* intermediates in ORR on platinum nanoparticles of various sizes.[117] This approach often provides results of comparable accuracy to the bilayer model. Of course, water clusters are very fluxional and are characterized by several local minima very close in energy.[119,120] Therefore, one needs to sample the potential energy landscape with sufficient accuracy in order to avoid overlooking relevant structures. A comparison between microsolvation, extended bilayer, and extended metal/water interface has been performed recently for the case of oxygenates on Pt(111).[121]

#### 7.2.2. Electrolyte

Electrochemical experiments are performed in solution and in the presence of an electrolyte to ensure charge balance. Although the counter-electrolyte is formally a spectator of the reaction, in some cases it can have a direct impact, as it can modulate the charge at the electrode and the consequent distribution of solvent molecules and availability of reactants in the active catalytic sites. A relevant example was recently reported in a joint experimental and theoretical study by the Koper and Lopez research groups, which shows that electroreduction of $CO_2$ on metal electrodes requires the presence of positive cations.[122] In this work $CO_2$ reduction was studied on gold electrodes and it was found that, without a metal cation, the reaction does not take place in a pure $H_2SO_4$ electrolyte. CO was produced on Cu, Ag or Au electrodes only when a metal cation was added to the solution. DFT calculations demonstrated that the metal cations stabilize the $CO_2^-$ intermediate via a short-range electrostatic interaction.

A further relevant example was reported by Bender et al.,[123] who provided a rationale behind the dependence of hydrogen production on the size of electrolyte cations. In particular it was shown that alkali metal cations have no systematic effect on HER rates in acid solutions while in alkaline media the reaction rates decrease with increasing cation size for Ir, Pd, and Pt ($Li^+ > Na^+ > K^+ > Cs^+$) and increase with cation size for Cu, Ag, and Au ($Li^+ < Na^+ < K^+ < Cs^+$). It was concluded that cations at the metal/electrode interface lower the activation barrier for water dissociation, a key step for HER in alkaline media. AIMD calculations helped to formulate the hypothesis that large, weakly solvated cations can better approach the electrode surface.

#### 7.2.3. Operando Conditions: pH, Voltage

Including pH and applied voltage in a simulation requires accounting for excess protons in the liquid water system and extra electrons at the electrode, respectively. Both problems have in common the need to consider extra charges. This can be done by explicitly simulating charged supercells neutralized either by using a homogeneous background of charge or by linearized or modified Poisson–Boltzmann equation, or by adopting alternative approaches, such as adding specific defects that inject extra charges into the catalytic environment keeping the overall system neutral. The first approach is more robust and does not induce any alterations to the chemistry of the examined systems, at the cost of requiring a Grand Canonical DFT formalism.[124,125] This is a general framework for treating electrochemical thermodynamics and kinetics as an explicit function of the electrode potential ($U$), temperature ($T$), and concentrations or, equivalently, (electro)chemical potentials ($\mu$). Specific applications of this approach to SACs have been reported.[126,127]

In this approach, protons can be explicitly added to the solvent environment and electrons are added to the electrode to mimic the working electrode potential. The addition of electrons causes a shift of the Fermi energy of the system, resulting in a specific applied potential, dependent on the concentration of added electrons. A relevant example was reported some time ago by Goddard and co-workers to explain the pH dependence of the HER.[124] Recently, Li and co-workers[128] and Wu et al.[129]

applied the methodology to $N_2$ electroreduction. For instance, in the work of Lee and co-workers the constant charge model (CCM) was compared to the constant potential model, which is more representative of a real electrochemical system. The comparison showed that, in the electrochemical processes, the exchange of electrons, ignored by the CCM, plays an important role in determining quantitatively the Gibbs free energy change, particularly at the potential-determining step.[128]

### 7.3. Intrinsic Stability of SACs

One important problem that is only rarely addressed when new SACs are considered based on electronic structure calculations is their overall stability in the reaction environment. In thermal catalysis the classical problem with isolated metal atoms as active sites is their diffusion and aggregation to form metal clusters and nanoparticles. Furthermore, in the long term, leaching/redeposition processes or amorphization of the support can occur, thus changing the structure of the catalyst. The other risk is that the system undergoes the phenomenon of strong metal support interaction, when part of the support migrates over the metal nanoparticle that becomes encapsulated in a more or less thin layer. This is particularly common when metal particles are supported on reducible oxides. A methodology to determine the thermodynamic stability of SACs compared to nanoparticles in the presence of adsorbates at a given pressure and temperature has been proposed recently.[130] The method is based on the graph-theoretical kinetic Monte Carlo approach where the DFT-calculated energies and vibrational frequencies are used as input using the software package Zacros.[131] The approach has been applied to the case of Pt(CO) units adsorbed on the $CeO_2$ surface and their diffusion to form (partially) CO-covered Pt nanoparticles, providing some indications on the conditions required to generate more stable catalysts.

Even more complex is the situation in electrocatalysis where the catalyst must survive rather harsh conditions of pH, oxidative or reducing environments under an applied external potential, interaction with metal ions dissolved in solution, etc. One approach to study the problem is to construct Pourbaix diagrams. These are plots showing the range of stability of various possible phases as a function of pH and applied potential. In this way the thermodynamic stability of various solid-state structures but also of ions in solution in different oxidation states is determined. Pourbaix diagrams have been generated also for SACs based on graphene structures, **Figure 4**, providing direct theoretical evidence that for Fe ions embedded in N-doped graphene demetallation is a dominant degradation mechanism under reactive conditions.[132]

### 7.4. Scaling Relations and Universal Descriptors

A powerful yet simple interpretative computational approach to rationalize the catalytic activity of several reactions of interest is based on the existence of scaling relations between chemical intermediates.[133] Scaling relations are correlations (often linear) that allow one to predict the free energies of all the remaining reaction intermediates in the catalytic cycle. They allow to reduce

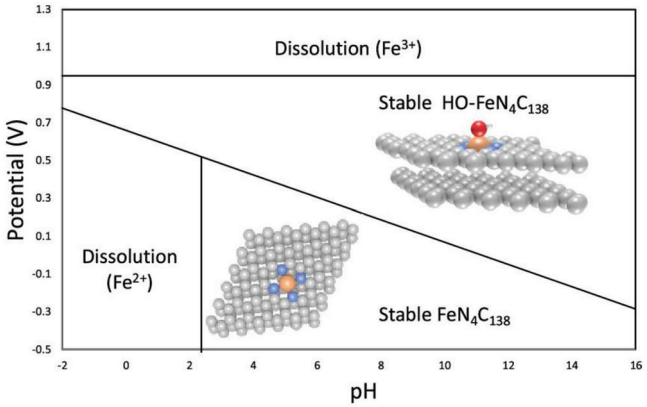


**Figure 4.** Stability diagram including $FeN_4C_{138}$, HO–$FeN_4C_{138}$, $Fe_{(aq)}^{2+}$ (1 M), and $Fe_{(aq)}^{3+}$ (1 M) phases at 298.15 K. Reproduced with permission.[132] Copyright 2020, American Chemical Society.

the complexity of the problem to the determination the activity of a few or even a single species, while the others are deduced from the scaling relations.

Inspired by this research, in the field of SACs a lot of attention has been devoted to the search for scaling relations.[134] However, the chemistry of SAC is complex as it is highly dependent on the local coordination as discussed above, and the reactivity is subject to the formation of several uncommon adducts. This makes the development of universal descriptors quite complex, although it opens at the same time the way to breaking linear scaling relationships.[135,136] For instance, theoretical simulations combined with experimental measurements have shown that the special properties of SACs and single-atoms alloys (SAAs) cannot be properly described by the scaling relations derived from the Brønsted–Evans–Polanyi (BEP) relationship that suggests a linear dependence between the reaction energy of a chemical process and its activation barrier. For instance, for numerous bond dissociation reactions SAAs combine weak binding and low activation, thus violating the traditional BEP relationships. The number of cases where a breaking of scaling relationships has been reported for SACs is surprisingly high.[136–138]

SAAs are particularly interesting systems. They usually consist of a coinage metal (Cu, Ag, and Au) doped, at the single-atom limit, with another metal. Based on DFT calculations, it has been shown that many surface alloys are resistant to cluster formation, and that they have a unique electronic structure with a very sharp d-band close to the Fermi level, reminiscent of the electronic structure of molecular species. These studies have been instrumental to discover and test experimentally new catalytic materials.[139,140]

The interest toward SACs and SAAs has stimulated an intense effort to search "universal" descriptors or direct correlations with observed properties in the attempt to define simple equations able to predict the behavior of an unknown catalyst using only some fundamental properties. This activity is facilitated by the use of machine learning (ML) algorithms[141] that allow one to explore large sets of data and to extract nonobvious relationships between the expected catalytic activity and some more or less elaborated descriptors.[142–144] The literature is full of

proposed equations of various complexity that have been obtained in this way. There are cases where the relations proposed are relatively simple. For instance, the HER activity of SACs consisting of TM atoms stabilized on $MoS_2$, $WS_2$, and $ZrS_2$ 2D materials has been shown to correlate with the electronegativity of the active site, of the neighboring atoms, and of their bond distances.[145] It should be mentioned, however, that the descriptors developed for this class of materials cannot be used for other systems, a problem of transferability that is common to several proposed descriptors.[86]

One problem with ML-derived descriptors is that they consist of rather complex formulas whose physical meaning is difficult to identify. Another problem is that often the descriptors are based on quantities that are not physical observables and must be obtained from DFT calculations (Bader charges, d-band center, etc.), thus making the whole descriptor method-dependent.

Thus, statistical learning techniques are very powerful and help the search for descriptors but often the black-box nature of these methods renders a physical interpretation difficult not to say impossible. While useful in principle to screen new potential catalysts, the number of variables, the complexity of the relations, and the fact that some quantities are not easily defined limits our understanding of the physical mechanisms that are at the basis of the chemical reactivity of a SAC. Despite intense efforts, the development of universal descriptors remains the holy grail in single-atom catalysis. Several papers have appeared in the literature where the identification of universal descriptors of SACs is claimed, also based on ML screening of large sets of data.[146–148] However, SACs are structurally and electronically too diverse to be described by a unique set of descriptors. It would not be surprising that universal descriptors of SACs simply do not exist.

## 8. Reactivity on SACs: Role of Nonclassical Intermediates

The concepts illustrated above will be used to discuss some reactions of particular relevance in our contemporary society. These are four processes that play a fundamental role in the energy transition and in the solution of critical environmental issues. We are referring to the two half-reactions involved in the splitting of water, the aforementioned HER and OER processes, and the activation and transformation by chemical reduction of two very stable molecules, $N_2$ to give ammonia or other hydrogenated species ($N_2$ reduction reaction, NRR) and $CO_2$ to give formaldehyde, methanol, methane or heavier hydrocarbons ($CO_2$ reduction reaction, CO2RR). The idea is not to provide detailed information about the four reactions, but rather to highlight the nature of the bonding of these molecules and the nature of reaction intermediates when the catalyst consists of single atoms. Since there are close similarities between SACs and coordination compounds and SACs are bridging homogenous and heterogeneous catalysis,[149] we begin by discussing how $H_2$, $O_2$, $N_2$, and $CO_2$ bind to transition metal complexes in comparison to extended metal surfaces, the active phase in many thermal catalysis and electrocatalysis processes.

### 8.1. Surface Chemistry versus Coordination Chemistry

#### *8.1.1. Hydrogen, $H_2$*

The first case we examine is also the simplest one. In fact, on metal surfaces $H_2$ can only exist in dissociated form or in a physisorbed state where the molecule is weakly bound to the surface via dispersion forces.[150] This means that also in the hydrogen evolution process H atoms diffuse on the surface until they recombine to form the $H_2$ molecule that immediately desorbs. Things are different in coordination compounds since here $H_2$ can interact with a TM atom forming dihydride or dihydrogen species.[151,152] In both cases two H atoms are bound to the TM center and, depending on the other ligands, the extent of charge transfer can be modulated so that it results in a complete breaking of the H—H bond, as in classical dihydride complexes TM(H)(H), or can be activated with an elongation of the H—H distance without complete dissociation, as in dihydrogen complexes TM($H_2$). In dihydrogen complexes the H—H distance is typically of 0.8–0.9 Å, i.e., slightly elongated with respect to the free molecule, 0.74 Å, while in dihydride complexes it can easily reach 2 Å or more.[153,154] This is a case where specific bonding situations can occur for TM complexes and also for SACs but not on extended surfaces or metal electrodes.[155,156]

#### *8.1.2. Oxygen, $O_2$*

The activation of $O_2$ on metal surfaces is relevant in heterogeneous catalysis, corrosion phenomena, passivation, etc. In general, the reactivity of a metal surface toward $O_2$ correlates with the O atom adsorption strength and the heat of formation of the oxide. There is a great variability of the reactivity of metal surfaces toward $O_2$. This is related to the degree of charge transfer to the antibonding orbitals of the $O_2$ molecule. For instance, on Au surfaces $O_2$ binds very weakly, the interaction is dominated by dispersion and the experimental desorption temperatures are very low, <55 K. Some metals such as Ag, Pd, and Pt can form both superoxo ($O_2^-$) and peroxo ($O_2^{2-}$) species, with net charge transfers to the adsorbed $O_2$ molecule, while on Ru and Ir only peroxo species have been observed. The most reactive metals are Rh, Co, and Fe, where molecularly adsorbed $O_2$ species are not observed due to the rapid dissociation into adsorbed O atoms, reflecting the rather low barriers for $O_2$ dissociation.[157]

Similar bonding modes are known to exist on TM complexes and are thus expected also for SACs. Needless to say that mononuclear metal–$O_2$ complexes have attracted great attention as these are key intermediates in the dioxygen activation by metalloenzymes.[158] Experimental data indicate a metal–superoxo TM($O_2^-$) or metal–peroxo TM($O_2^{2-}$) intermediate, depending on the amount of charge transfer. Larger O–O distances and lower O–O frequencies are expected for peroxo than for superoxo complexes and are used to discriminate the two forms. $O_2$ can bind in a bent end-on fashion, more typical for superoxo ($O_2^-$) species, or in side-on mode, indicative of the formation of a peroxo complex, but intermediate situations are also known.[159,160]

A brief comment is in order when one considers the total energy of the $O_2$ gas-phase molecule as determined from DFT

calculations. GGA functionals tend to severely overestimate the O—O bond strength by ≈20%, a problem that is solved by the use of hybrid functionals.[161] Sargeant et al. have shown for the case of the oxygen reduction and evolution reactions (ORR and OER) that the use of semiempirical corrections for gas-phase $O_2$ is dangerous.[162] The error due to oxygen may affect not only the overall equilibrium potential of the reaction, but also the energies of individual mechanistic steps.

#### 8.1.3. Nitrogen, $N_2$

$N_2$ adsorbs in different states on the surfaces of transition metals. Physisorbed $N_2$ is formed only at very low temperatures, <50 K, while in the chemisorbed state the $N_2$ molecule can bind with the N–N axis normal to the metal surface (terminal end-on) or assuming a side-on orientation. In this case both the N atoms form a chemical bond with the surface generating a precursor state of the dissociative adsorption. This hardly occurs on the regular surface sites, while it is possible on low-coordinated atoms at steps, as shown for the case of steps created on the Ru(0001) surface.[163]

The first example of a dinitrogen complex with a TM was reported in 1965 for a Ru species.[164] Since then other examples have been reported where the $N_2$ molecule is bound in a variety of modes, with two dominating configurations, end-on and side-on, in analogy with the metal surfaces. These two modes result in different reaction pathways when involved in reduction processes. For instance, end-on $N_2$ ligands can be protonated at the terminal N atom, where the resulting TM(NNH) intermediate is the first step in a series of reductions and protonations at the distal nitrogen leading to ammonia and a metal nitride TM≡N. This mechanism is inhibited if $N_2$ binds in a side-on mode. On the other hand, the N—N side-on bonding mode is the precursor state of the direct NN bond cleavage to form two TM≡N nitride complexes.[165,166]

#### 8.1.4. Carbon Dioxide, $CO_2$

On most low-index metal surfaces $CO_2$ binds only very weakly through dispersion forces. Defected, stepped, or alkali metal precovered metal surfaces, thanks to lower work functions, are more reactive as they are able to transfer charge to adsorbed $CO_2$. Three main coordination geometries for the $CO_2$ molecule can be identified, (a) pure carbon coordination, (b) pure oxygen coordination, (c) mixed carbon—oxygen coordination. Dissociation of $CO_2$ has been reported on powders, stepped Cu surfaces, reactive Ni surfaces and a few other systems. On some of these surfaces the molecule can assume nonlinear structures, indicative of the formation of a $CO_2^{\delta-}$ species, which can be considered as a precursor to carbonate formation. Coadsorption of $CO_2$ and oxygen leads to carbonate formation on some metal surfaces.[167–170]

The relations between the bonding modes of $CO_2$ on metal surfaces and TM complexes have been discussed in the past.[171] On TM complexes the $CO_2$ molecule exhibits several distinct positions: see **Figure 5**.

The $\eta^1$(C) and $\eta^2$(C,O) side-on coordination modes have been confirmed by X-ray crystal structure determinations of known metal $CO_2$ complexes, e.g., $[Rh(diars)_2(Cl)(\eta^1\text{-}CO_2)]$, $[Ni(\eta^2\text{-}CO_2)(PCy_3)_2]$, and $[Cp'_2Nb(\eta^2\text{-}CO_2)(CH_2SiMe_3)]$.[172] No X-ray crystal structural data were available of the $\eta^1$(O) coordination mode until a complex in which the $CO_2$ ligand is linearly coordinated to a uranium complex was reported.[173] Of course, $CO_2$ can also bind to two or more metal centers via coordination of C to one metal and either one or both of the O atoms of the $CO_2$ to other metal(s). This however can be reproduced only when two metal centers are simultaneously present as in bimetallic complexes or dual-atom catalysts (DACs).

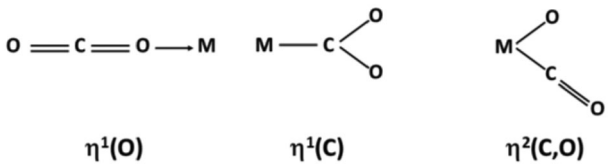


**Figure 5.** Bonding modes of $CO_2$ to TM complexes.

### 8.2. Reactions on SACs Relevant for the Energy Transition

In the following we will discuss four examples of relevant reactions that may be catalyzed by SACs. These reactions have been chosen because they provide very useful examples of how the activation and conversion of $H_2$, $O_2$, $N_2$, and $CO_2$ on SACs occurs with formation of adsorbed complexes and reaction intermediates that have strong analogies with corresponding coordination compounds. The other important message emerging from the analysis of the four reactions, HER, OER, NRR, and CO2RR, is that the modeling of the reaction path must consider all possible intermediates and not only those that normally occur on the surface of metal electrodes: the chemistry of SACs in fact is markedly different from that of extended metal surfaces.

#### 8.2.1. HER

In standard conditions, the semireaction $2\,H^+ + 2\,e^- \rightarrow H_2$ is associated with a change of Gibbs free energy, $\Delta G^0$, equal to zero, Equation (1). Thus, the potential required to promote the reaction is also zero, as $\Delta G^0 = -nFE^0$ where $n$ is the number of electrons involved, $F$ the Faraday's constant, and $E^0$ the reduction potential. Under real conditions, an overpotential $\eta$ is required for the reaction to occur but it is generally assumed that $\eta = 0$, which is of course a very crude approximation.

On a metal electrode the reaction is

$$H^+ + e^- + * \rightarrow H* \tag{2}$$

where H* denotes an adsorbed H atom on the metal surface. This is known as Volmer step. To form $H_2$ the reaction can follow two different paths. According to the Heyrovsky mechanism a second proton is reduced on the same metal site

$$H* + H^+ + e^- \rightarrow * + H_2 \tag{3}$$

The second possibility, the Tafel mechanism, implies that two adsorbed H* atoms diffuse and recombine to form $H_2$

$$2H* \rightarrow 2* + H_2 \tag{4}$$

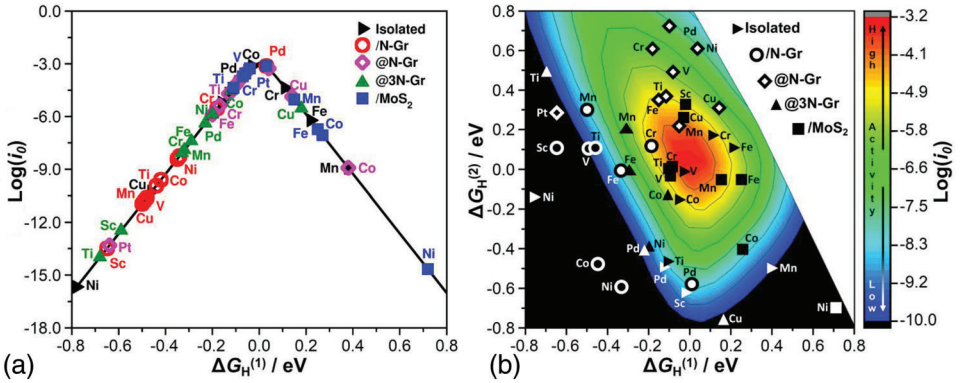


**Figure 6.** a) 2D volcano plot derived from DFT results for the HER on 55 SACs computed assuming the formation of a H* intermediate. b) 3D volcano plot derived from DFT results for the HER on 55 SACs assuming the formation of both H* and H*H* (dihydrogen) intermediates. Red: high activity; blue: low activity. When $\log(i_0) < -10$ (extremely low activity) the color is black. Reproduced under the terms of the CC-BY Creative Commons Attribution 4.0 International license (https://creativecommons.org/licenses/by/4.0).[155] Copyright 2021, The Authors, published by American Chemical Society.

Both paths are relevant and may occur at the same time, their predominance depending on the hydrogen coverage.[174]

Once formed, the $H_2$ molecule interacts weakly with the surface via dispersion forces and is released to the gas-phase at finite temperatures. Since the physisorbed intermediate is practically at the same energy of the separated systems, M + $H_2$, this minimum in the potential energy surface can be ignored and the $\Delta G^0_H$ of the reaction can be computed using a single descriptor, the strength of the M—H bond. This leads to a volcano curve, **Figure 6**a, where the exchange current, $i_0$, of the HER is plotted against the M—H bond strength, as proposed by Trasatti 50 years ago (the exchange current is proportional to the amount of $H_2$ produced).[175]

Thus, the activity of a catalyst, as measured by the exchange current $i_0$, can be predicted simply by evaluating the adsorption energy of a H atom on a metal surface, $\Delta E_H$, and deriving the corresponding Gibbs free energy

$$\Delta G^0_H = \Delta E_H + \Delta E_{ZPE} - T\Delta S^0_H \quad (5)$$

The catalysts that are on the top of the resulting volcano plot are the best ones since they correspond to the ideal condition $\Delta G^0_H = 0$, i.e., to catalysts that bind H not too strongly nor too weakly, Figure 6a. Recently it has been shown that a small correction is required and that at $\eta > 0.10$ V optimal catalysts have $\Delta G^0 \approx +0.2$ eV).[176]

This approach is perfectly valid and has been successfully applied to the theoretical study of several metal catalysts.[41,177–179] The very same approach has been used, without change, to study and interpret the activity of known SACs or, more frequently, to predict the performances of new SACs not yet synthesized. In all these studies the original CHE model developed for extended metal surfaces has been adopted, without considering that the chemistry of SACs can be markedly different from that of an extended metal surface.

We already mentioned that TM complexes can bind two H atoms, forming stable dihydrogen or dihydride complexes (see Section 8.1.1). Recently it has been shown that similar stable intermediates can form on SACs, a result that is not too surprising in view of the already mentioned analogies of SACs and coordination compounds.[155] However, when the formation of dihydrogen complexes occurs, it has major consequences on the reaction profile and on the kinetics of the reaction. In fact, this means that besides the H* intermediate usually considered (an isolated H atom bound to the active center), associated with a $\Delta G^0_{H(1)}$, one has to consider the free energy change for the adsorption of the second H atom in the H*H* dihydrogen complex, $\Delta G^0_{H(2)}$

$$H^+ + e^- + H* \rightarrow H*H* \quad (6)$$

The last reaction step, $H_2$ evolution

$$H*H* \rightarrow * + H_2 \quad (7)$$

is thus function of two variables, $\Delta G^0_{H(1)}$ and $\Delta G^0_{H(2)}$

$$\Delta G^0_{H(3)} = \Delta G^0_{H(1)} + \Delta G^0_{H(2)} \quad (8)$$

This leads to a 3D volcano plot, Figure 6b, and to the fact that many catalysts that are predicted to be active when only the H* intermediate is considered, are indeed inactive or moderately active when the formation of the second H*H* intermediate is considered, Figure 6b. Thus, the theoretical study of the HER on SACs requires to consider two formation energies, and not just one as it is usually done.

This example shows that: 1) SACs have a different and richer chemistry that that of extended metal surfaces, and 2) only if all reaction intermediates are considered one can reasonably expect to be able to predict the activity of a SAC. In the following we will show that this is not restricted to the HER, but is a general message valid for every chemical process.

### 8.2.2. OER

The OER is the oxidation semireaction of water splitting. It is generally assumed that on metal electrodes the reaction occurs via formation of three intermediates, each one releasing one electron[87]

$$H_2O + * \rightarrow OH^* + H^+ + e^- \quad (9)$$

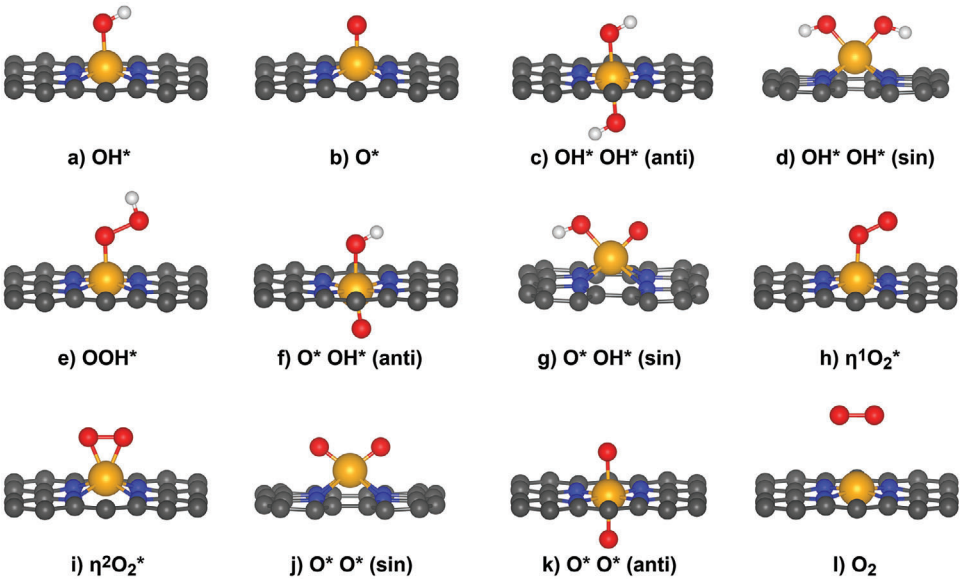


**Figure 7.** Possible OER intermediates on SACs embedded in 2D carbon nanostructures. Reproduced with permission.[184] Copyright 2023, Elsevier.

$$OH^* \rightarrow O^* + H^+ + e^- \quad (10)$$

$$H_2O + O^* \rightarrow OOH^* + H^+ + e^- \quad (11)$$

In the last step a fourth electron is released, with formation of $O_2$

$$OOH^* \rightarrow * + O_2 + H^+ + e^- \quad (12)$$

Notice that on oxide surfaces (NiOOH, CoOOH, $IrO_2$ or $RuO_2$) the mechanism can be different and deviate from this assumption. As for the HER, also the OER can be modeled by evaluating the Gibbs free energies of each intermediate and neglecting any other reaction barrier, although attempts to include kinetic effects in similar processes have been reported.[180] Also in this case, the formation of the "classical" OH*, O*, and OOH* intermediates has been assumed when dealing with SACs, thus extending with no modifications the traditional model used for metal surfaces.[181,182] However, the chemistry of SACs toward O-containing molecular fragments is even richer than that of the same systems in the HER. As shown by various studies in coordination chemistry, several other species can form when the active site consists of a single TM atom. For instance, after formation of the OH* complex, Equation (9), a second hydroxyl group can bind to the metal center, leading to two bound OH groups, OH* OH*, **Figure 7**[183,184]

$$2H_2O \rightarrow OH^*OH^* + 2H^+ + 2e^- \quad (13)$$

This complex, which implies the release of two electrons, is an alternative to the formation of the O* intermediate that is normally considered in all studies on the reactivity of SACs. The formation of the unconventional OH* OH* intermediate can proceed following the classical path, i.e., leading to the formation of the standard OOH* intermediate

$$OH^*OH^* \rightarrow OOH^* + H^+ + e^- \quad (14)$$

or can follow another path with formation of an OH* O* complex where an OH group and an O atom are simultaneously bound to the TM[185]

$$OH^*OH^* \rightarrow OH^*O^* + H^+ + e^- \quad (15)$$

Thus, the OOH* and the OH* O* intermediates are alternative possibilities that imply different reaction paths (notice that in both cases the step involves the release of three electrons). No matter if the reaction follows the classical OOH* step or the unconventional OH* O* one, the next step implies the formation of peroxo or superoxo $O_2$* complexes

$$OH^*O^* \rightarrow O_2^* + H^+ + e^- \quad (16)$$

$$OOH^* \rightarrow O_2^* + H^+ + e^- \quad (17)$$

These species can form on SACs in full analogy with coordination chemistry compounds, introducing an additional step before release of $O_2$. This step is usually neglected in the modeling of OER on SACs.[186] This partial and incomplete list of the possible intermediates shows that, as for the HER, also for the OER the formation of the new stable species on SACs has important effects on the kinetics of the process.

To show how the formation of the new intermediates complicates the picture, we report in **Figure 8** a summary of the possible reaction mechanisms with the classical path based on the OH*, O*, and OOH* intermediates in red; in blue and green are shown the alternative paths that include the other possible intermediates. Needless to say, only if the entire mechanism of the

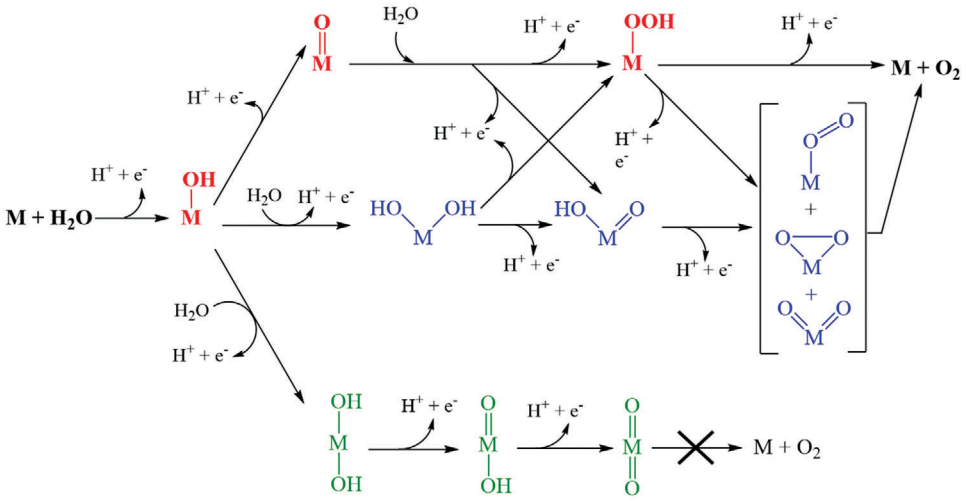


**Figure 8.** Oxygen evolution reaction (OER) scheme were all the possible pathways are showed. Red: classical path based on the OH*, O*, and OOH* intermediates. Blue and green: alternative paths that include the other possible intermediates. Reproduced with permission.[184] Copyright 2023, Elsevier.

reaction is properly explored one can formulate reliable suggestions for the expected reactivity of unknown SACs.

### *8.2.3. NRR*

The production of ammonia ($NH_3$) from nitrogen ($N_2$) is probably the most important chemical process that has been developed so far. Today the industrial production of ammonia is still based on the Haber–Bosch process where $N_2$ and $H_2$ react at high temperatures and pressures according to the classical reaction $N_2(g) + 3H_2(g) \rightarrow 2NH_3(g)$. The process occurs on Fe-based bulk catalyst and is responsible for 1–2% of worldwide energy consumption. Hydrogen is produced via methane steam reforming and this is also responsible for the large energy input required for the reaction.

In nature, $NH_3$ is synthesized thanks to the enzyme nitrogenase. Differently from the industrial process, enzymes are able to produce ammonia under ambient conditions, although the process is not very efficient from an energy point of view.[187] The overall reaction implies the transfer of 3 electrons per N atom

$$N_2 + 6\left(H^+ + e^-\right) \rightarrow 2NH_3 \quad (18)$$

Clearly, the enzymatic and electrochemical routes to the ammonia synthesis are markedly different from that of the Harber–Bosh process. In particular, in the Haber–Bosch process the rate determining step is the $N_2$ (and $H_2$) dissociation, a process that implies very high energy barriers (dissociative mechanism); then, the N and H atoms diffuse on the surface of the catalyst, recombine and lead to desorption of the final $NH_3$ product. On the contrary, in electrocatalytic reduction the $N_2$ molecules are sequentially hydrogenated (associative mechanism) with consequent weakening of the N—N bond that thus requires much less energy in order to be dissociated. The electrochemical reduction of $N_2$ to ammonia (NRR) is a potential alternative to thermal catalysis (Haber–Bosch).

In this respect, SACs represent ideal systems to study potential alternatives to enzymatic catalysis for the electrochemical synthesis of ammonia, and a large number of studies have been dedicated to the problem, also from the theory point of view.[188,189] There are also specific reasons why SACs represent interesting alternatives to classical metal catalysts for the reaction. One is that they can efficiently suppress HER, the alternative process to NRR. For instance, SACs can have more positive $\Delta G_{H^*}$ than most metal surfaces, making HER less favorable with considerable improvements in the NRR/HER selectivity.[190] Furthermore, several SACs show highly negative $\Delta G_{N2^*}$, an effect that has been attributed to the positive oxidation state of TMs and the consequent effective polarization of the adsorbed $N_2$ molecule.

As we mentioned before, the entire NRR process includes six proton-coupled electron-transfer steps, and the study of the reaction requires to consider all possible reaction pathways and compute the corresponding Gibbs free-energy changes. For each adsorption form of the $N_2$ molecule, end-on or side-on, two possible reaction mechanisms must be considered, the distal (**Figure 9**a) and alternating (Figure 9b) mechanisms for the end-on structures and the consecutive (Figure 9c) and enzymatic (Figure 9d) mechanisms for side-on ones. In the distal and consecutive mechanisms, the proton–electron pairs sequentially attack one nitrogen atom to form the first $NH_3$ molecule and only then attack the other nitrogen atom to form the second $NH_3$ molecule. On the contrary, for the alternating and enzymatic mechanisms, the proton–electron pairs alternatively attack the two nitrogen atoms. The first two steps along all pathways, i.e., $N_2$ adsorption and activation and first protonation with the formation of $N_2H^*$, are the same.

General conditions for the good performance of SACs in NRR are: 1) the capability to absorb $N_2$ spontaneously and 2) the fact that often $\Delta G_{N2^*}$ is more negative than $\Delta G_{H^*}$, thus showing good selectivity for NRR against the competitive HER. Furthermore, the potential limiting steps of electrocatalytic NRR are the first protonation, $N_2^* + (H^+ + e^-) \rightarrow N\text{–}NH^*$, and the last protonation, $NH_2^* + (H^+ + e^-) \rightarrow NH_3^*$. Thus, good SACs for NRR should be able to stabilize the $N_2H^*$ intermediate and destabilize the $NH_2^*$ one to reduce the overpotential. It has been shown that the number of unpaired electrons and in general the

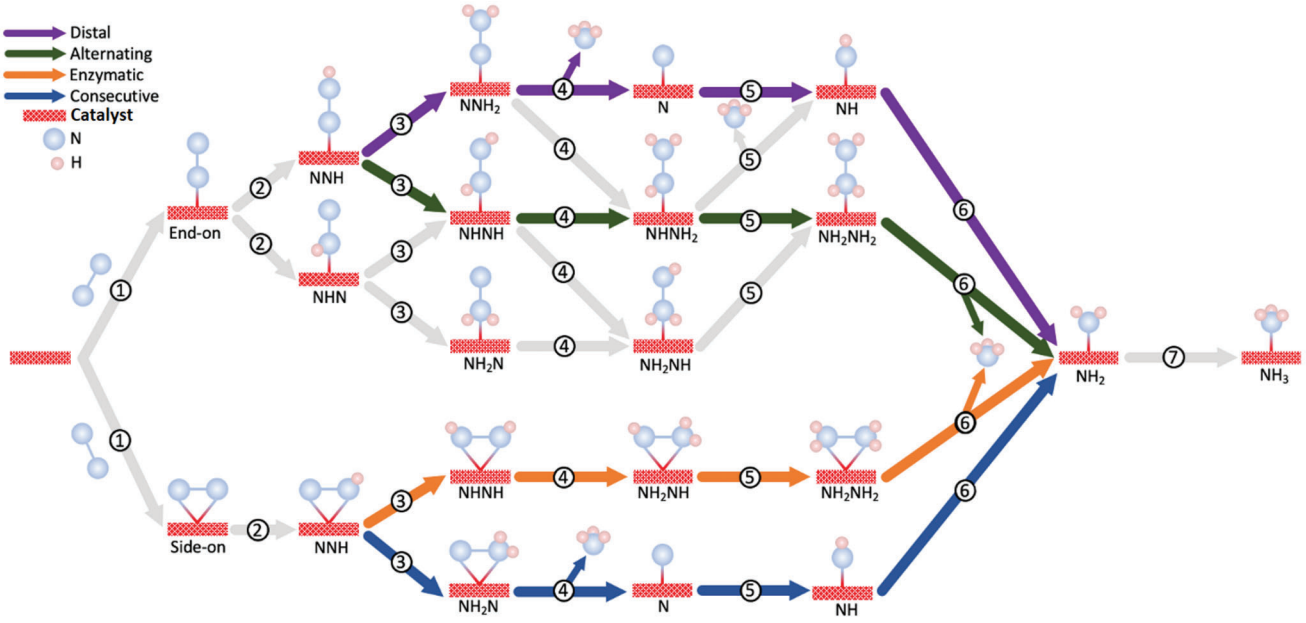


**Figure 9.** Distal, alternating, consecutive, and enzymatic mechanisms for the NRR.

occupation of d orbitals of the TM atom determines the "acceptance-donation" mechanism.[191,192] The possibility to tune this quantity by playing around with TM atoms embedded in various matrices opens the possibility to find particularly well suited systems for NRR and makes SACs particular attractive for the design of new catalytic systems able to mimic the enzymatic process.

### 8.2.4. CO2RR

In nature, $CO_2$ is converted to sugars or carbohydrates and oxygen via the process of photosynthesis thanks to the energy provided by solar light in a series of complex chemical steps. The processes that mimic carbon fixation are known as artificial photosynthesis. The chemical reduction of $CO_2$ via thermal catalysis or electrocatalysis is one of the most studied processes for the sustainable production of synthetic and solar fuels. The difficulty of the reaction is related to the high thermodynamic stability of the $CO_2$ molecule, and the even higher potential required to reduce $CO_2$ to $CO_2^-$ (−1.90 V vs SHE at pH = 7). The process to reduce $CO_2$ to C1 chemicals (CO, $CH_3OH$, $CH_4$) occurs in a rather complex sequence of steps, and is kinetically hindered, with high barriers involved in the formation of the intermediates. In general, there are two possible alternative mechanisms for the reaction, one where the adsorbed $CO_2$ molecule binds via C and H atom to form the formate intermediate (HCOO*). In thermal catalysis the H atom is supposed to derive from the dissociation of gas-phase $H_2$ molecules on other sites of the catalysts; in electrocatalysis HCOO* forms by the addition of a proton $H^+$ and an electron $e^-$ to the activated $CO_2$ molecule. The reaction is followed by several steps before methanol or methane are released.[193]

The alternative to the formate mechanism proceeds via dissociation of the activated $CO_2$ molecule. By interacting with H atoms, $CO_2$ is first converted to CO and $H_2O$. In thermal catalysis this is known as the reverse water gas-shift reaction; in electrocatalysis the typical chemical equations are

$$CO_2\,(g) + 2H^+ + 2e^- \rightarrow CO\,(g) + H_2O\,(l)\ \text{(acidic media)} \quad (19)$$

or

$$CO_2\,(g) + 2H_2O\,(l) + 2e^- \rightarrow CO\,(g) + 2OH^-\ \text{(nonacidic media)} \quad (20)$$

Then CO is further hydrogenated to formyl, HCO*, and formaldehyde HCHO* intermediates.

Examples of CO2RR based on SACs have been reported and corroborated or complemented by computational studies.[194,195] Of course, several screening studies have also been performed to predict ideal catalysts based on single metal atoms.

Differently from the HER or the OER processes, the intermediates that are usually discussed and considered in the theoretical analysis of the CO2RR are the same on classical solid catalysts based on extended metal electrodes, on supported metal particles, or on SACs. Formate, HCOO*, and CO* are the two classical products of the initial reduction of $CO_2$. What is less discussed in the theoretical literature, however, is the bonding and activation of the $CO_2$ molecule to the active site. Due to the already mentioned high thermodynamic stability, $CO_2$ is rather unreactive and binds weakly to several supports. In thermal catalysis the problem can be overcome by increasing the $CO_2$ partial pressure. In electrocatalysis, where the reaction occurs in a solvent, usually water, the bonding and activation of the molecule to the active site becomes essential. If the $CO_2$ molecule does not stick to the catalytic center, the reaction will hardly occur. This problem is often neglected in the theoretical discussions. The state corresponding to adsorbed $CO_2$* is taken as the zero reference for the Gibbs

free energy of the process, without discussing the stability of the $CO_2$* species under the normal reaction conditions.

In this respect, it is important to mention that when the reaction occurs in water, another phenomenon can take place that is largely (not to say totally) ignored in the literature on the subject. Water molecules not only can solvate the reactants and intermediates, leading to changes in the computed barriers and thermodynamic quantities, but can also act as ligands themselves, binding to the active metal center via electrostatic forces (when the TM is in a positive oxidation state) or via more covalent interactions. Recently, it has been shown that $H_2O$ molecules can bind to SACs with bond strengths that are comparable or can even exceed that of the reactant, in this case a $CO_2$ molecule.[196] This means that the $CO_2$ molecule not only must bind sufficiently strongly to the active site in order to be activated, but must also displace solvent molecules that can block the active site.

This problem represents another manifestation of the similarity between SAC and organometallic complexes. The final message of this discussion is therefore that while SACs, at a superficial analysis, appear to be simpler than other catalytic systems such as supported metal particles, in reality their chemistry is complex and rich, and their modeling requires including a series of factors and aspects often overlooked, with possible effects on the reliability of the predictions.

## 9. Summary and Conclusions

The continuous growth of powerful computers associated to the impressive development of accurate methods to solve the Schrödinger equation for complex systems offer today the opportunity to simulate with desired accuracy the chemistry of molecular and solid-state systems. It is not surprising that this approach has been used to better understand and predict the properties of single-atom catalysts, a very promising branch of heterogeneous catalysis with interesting connections with homogeneous catalysis.

In the last few years, we have assisted to the explosion of screening studies of the catalytic activity of large numbers of unknown and potentially interesting materials where isolated transition metal atoms are bound to supporting matrices. These include bulk oxides, single-layer graphene, 2D metal dichalcogenides, covalent organic frameworks, etc. In principle the production of large databases of computed properties can be useful in the context of using ML algorithms to derive nonobvious correlations or novel descriptors of the activity of a catalyst. This intense activity is intended to facilitate the work of experimentalists in selecting the most promising systems without wasting time in the attempt to synthesize and characterize catalysts that are not expected to be active for a given reaction.

This effort can lead to positive developments provided that the results produced by the simulations are reliable, realistic, and verifiable. Simulating a SAC and its catalytic performance is less trivial than often believed and requires including many important factors and effects that contribute to the final activity. Without this, it is doubtful that the simulation will produce useful results, and if it does it is probably fortuitous.

In this brief *Perspective* we have analyzed some of the most common limitations and drawbacks of computational studies on the nature and activity of SACs. We began by mentioning the importance of knowing precisely the local coordination of the active site, as this is essential for determining the chemistry of the system. It turns out that even the most advanced characterization methods often fail to give an accurate description of the catalyst structure at the atomistic level. Even modest changes in the surrounding environment of the active site can result in large changes in activity. Furthermore, SACs are not static entities and can change their structure during the course of the reaction. These aspects should be carefully considered when comparing the theoretical with the experimental results.

We mentioned the importance of the choice of the DFT approach in determining the quality of the final results. Most of the calculations of SACs are based on semilocal GGA functionals. These are good (although not perfect) for extended metals, but have serious limitations when applied to systems with localized electronic states, as is the case of TM atoms in a surrounding matrix. The differences can be substantial. For instance, the binding energy of an adsorbate on the active site can change by 0.5 eV or more by changing the exchange-correlation functional, with qualitative, and not only quantitative, effects on the final results. The use of hybrid functionals or of DFT+$U$ methods is highly recommended to reduce this kind of inaccuracies. In general, it is good praxis to compare results obtained with different functionals.

Next, we moved to the essential ingredients that are required to construct a reliable model of an actual SAC. The general assumption in virtually all simulation studies on SACs, in particular in electrocatalysis, is that one can take a thermodynamic approach where the calculation of the stability of the intermediates provides an acceptable estimate of the reaction profile. In this approach, only the thermodynamic barriers are considered, while the activation energies separating two intermediates are assumed to be negligible, an approximation that can considerably affect the reaction kinetics.

More severe are other approximations usually done in the simulation of SACs. Electrocatalysis occurs in water, and the inclusion of the solvent in the model can alter the adsorption energies and the stability of the reaction intermediates. For some reactions there is evidence that the role of solvation is modest and can be neglected, but there also cases where this is no longer true. The solvent can be described in various ways, but dynamic aspects of liquid water can be very important in determining the structure at the solid/liquid interface. Furthermore, water can act as a ligand itself, competing with reactants, products or intermediates in bonding to the active site.

There are other effects that are usually neglected and that can be relevant, and sometimes even crucial. This is the case of ions in solution and their concentration, of the pH, and of the applied voltage. The presence of the electrolyte and the density of hydrogen ions have been shown to be determinant in specific cases. While it is possible that for some reactions these effects do not change the general picture, it is good practice to verify this before performing screening studies of electrochemical reactions.

A key problem very rarely addressed in computational screening studies is the stability of the predicted structures. It is not uncommon to find studies where numerous systems are investigated for their potential activity without assessing if these can survive the harsh working conditions of the experimental studies. It is well known that one of the most important aspects in catalysis is, beside the activity, the long-term stability and the resistance

to sintering and corrosion of the catalyst. In order to be useful, the prediction of new catalysts should also address the question of stability in aggressive environments as that of electrocatalytic processes or of thermal catalysis at high temperatures and pressures.

Finally, we have revisited some relevant processes, HER, OER, NRR, and CO2RR, to show that on SACs these proceed via reaction paths that can differ substantially from those found on metal electrodes. In particular, due to the similarity of SACs with coordination compounds, several new intermediates can form on SACs that do not form on metal surfaces. When this occurs the kinetics of the reaction is heavily affected. Predictions of catalytic activity based on subsets of reaction intermediates have little meaning and a high probability to be incorrect.

This incomplete list of aspects shows how delicate and complex is the theoretical description of these systems. This complexity is often underestimated. Unless these effects lead to fortuitous error cancellations, something that has not been demonstrated so far, one cannot expect reliable predictions of catalytic activity from simulations that do not include important effects or do not use the appropriate methods. The production of large set of data of low-accuracy can also be detrimental when these data are used to train ML algorithms or to derive trends or descriptors.

The bottom line is that electronic structure calculations are very powerful tools provided the key ingredients of a process are included into the model used. Oversimplified models can be of interest only after it has been shown that the approximations made are justified and do not alter the general conclusions. Generating large sets of data of dubious accuracy on potentially interesting catalytic systems risks creating distrust of the field more than being beneficial to the experimentalists. The arsenal of methods and computer codes available today to theorists allows one to perform reliable calculations using realistic models. Yet, there is still room for improvement. The cost of post-Hartree–Fock calculations for periodic systems remains very high and exchange-correlation functionals are still susceptible to significant (system dependent) errors. This represents a stimulus for the theoretical community to develop even more accurate and powerful tools to predict the behavior of complex materials in catalysis.

## Acknowledgements

The authors thank I. Barlocco, L. A. Cipriano, L. Giordano, V. Caruggi, M. Spotti, F. Maleki, D. Misra, H. V. Thang, and S. Tosoni for useful discussions. Access to the CINECA supercomputing resources was granted via ISCRAB. The authors also thank the COST Action 18234 supported by COST (European Cooperation in Science and Technology).

Open Access Funding provided by Universita degli Studi di Milano-Bicocca within the CRUI-CARE Agreement.

## Conflict of Interest

The authors declare no conflict of interest.

## Keywords

electrocatalysis, electronic structure theory, quantum chemical simulations, single-atom catalysis

Received: July 19, 2023
Revised: August 17, 2023
Published online: September 25, 2023

[1] F. Haber, R. Le Rossignol, *J. Ind. Eng. Chem.* **1913**, *5*, 328.
[2] Y. Lou, J. Xu, Y. Zhang, C. Pan, Y. Dong, Y. Zhu, *Mater. Today Nano* **2020**, *12*, 100093.
[3] M. Boudart, *Adv. Catal.* **1969**, *20*, 153.
[4] A. A. Herzing, C. J. Kiely, A. F. Carley, P. Landon, G. J. Hutchings, *Science* **2008**, *321*, 1331.
[5] G. Pacchioni, H.-J. Freund, *Chem. Soc. Rev.* **2018**, *47*, 8474.
[6] *Nanocatalysis* (Eds: U. Heiz, U. Landman), Springer, Berlin, Germany **2007**.
[7] Z. Luo, A. W. Castleman, S. N. Khanna, *Chem. Rev.* **2016**, *116*, 14456.
[8] U. Landman, B. Yoon, C. Zhang, U. Heiz, M. Arenz, *Top. Catal.* **2007**, *44*, 145.
[9] E. Arlman, *J. Catal.* **1964**, *3*, 99.
[10] A. K. Smith, B. Besson, J. M. Basset, R. Psaro, A. Fusi, R. Ugo, *J. Organomet. Chem.* **1980**, *192*, C31.
[11] P. Serna, B. C. Gates, *Acc. Chem. Res.* **2014**, *47*, 2612.
[12] C. Copéret, A. Comas-Vives, M. P. Conley, D. P. Estes, A. Fedorov, V. Mougel, H. Nagae, F. Núñez-Zarur, P. A. Zhizhko, *Chem. Rev.* **2016**, *116*, 323.
[13] M. K. Samantaray, V. D'Elia, E. Pump, L. Falivene, M. Harb, S. Ould Chikh, L. Cavallo, J.-M. Basset, *Chem. Rev.* **2020**, *120*, 734.
[14] M. K. Samantaray, E. Pump, A. Bendjeriou-Sedjerari, V. D'Elia, J. D. A. Pelletier, M. Guidotti, R. Psaro, J.-M. Basset, *Chem. Soc. Rev.* **2018**, *47*, 8403.
[15] K. Asakura, H. Nagahiro, N. Ichikuni, Y. Iwasawa, *Appl. Catal., A* **1999**, *188*, 313.
[16] S. Abbet, A. Sanchez, U. Heiz, W.-D. Schneider, A. M. Ferrari, G. Pacchioni, N. Rösch, *J. Am. Chem. Soc.* **2000**, *122*, 3453.
[17] Q. Fu, H. Saltsburg, M. Flytzani-Stephanopoulos, *Science* **2003**, *301*, 935.
[18] J. Lu, P. Serna, B. C. Gates, *ACS Catal.* **2011**, *1*, 1549.
[19] A. S. Hoffman, L. M. Debefve, S. Zhang, J. E. Perez-Aguilar, E. T. Conley, K. R. Justl, I. Arslan, D. A. Dixon, B. C. Gates, *ACS Catal.* **2018**, *8*, 3489.
[20] B. Qiao, A. Wang, X. Yang, L. F. Allard, Z. Jiang, Y. Cui, J. Liu, J. Li, T. Zhang, *Nat. Chem.* **2011**, *3*, 634.
[21] V. Hasija, S. Patial, P. Raizada, A. Aslam Parwaz Khan, A. M. Asiri, Q. Van Le, V.-H. Nguyen, P. Singh, *Coord. Chem. Rev.* **2022**, *452*, 214298.
[22] G. Vilé, G. Di Liberto, S. Tosoni, A. Sivo, V. Ruta, M. Nachtegaal, A. H. Clark, S. Agnoli, Y. Zou, A. Savateev, M. Antonietti, G. Pacchioni, *ACS Catal.* **2022**, *12*, 2947.
[23] H. Fei, J. Dong, D. Chen, T. Hu, X. Duan, I. Shakir, Y. Huang, X. Duan, *Chem. Soc. Rev.* **2019**, *48*, 5207.
[24] M. B. Gawande, P. Fornasiero, R. Zbořil, *ACS Catal.* **2020**, *10*, 2231.
[25] D. Van Dao, L. A. Cipriano, G. Di Liberto, T. T. D. Nguyen, S.-W. Ki, H. Son, G.-C. Kim, K. H. Lee, J.-K. Yang, Y.-T. Yu, G. Pacchioni, I.-H. Lee, *J. Mater. Chem. A* **2021**, *9*, 22810.
[26] D. Van Dao, G. Di Liberto, H. Ko, J. Park, W. Wang, D. Shin, H. Son, Q. Van Le, T. Van Nguyen, V. Van Tan, G. Pacchioni, I.-H. Lee, *J. Mater. Chem. A* **2022**, *10*, 3330.
[27] H. Oschinski, Á. Morales-García, F. Illas, *J. Phys. Chem. C* **2021**, *125*, 2477.
[28] L. Jiao, H. Yan, Y. Wu, W. Gu, C. Zhu, D. Du, Y. Lin, *Angew. Chem., Int. Ed.* **2020**, *59*, 2565.
[29] L. Huang, J. Chen, L. Gan, J. Wang, S. Dong, *Sci. Adv.* **2019**, *5*, 5490.
[30] M. A. Bajada, J. Sanjosé-Orduna, G. Di Liberto, S. Tosoni, G. Pacchioni, T. Noël, G. Vilé, *Chem. Soc. Rev.* **2022**, *51*, 3898.

[31] M. A. Bajada, G. Di Liberto, S. Tosoni, V. Ruta, L. Mino, N. Allasia, A. Sivo, G. Pacchioni, G. Vilé, *Nat. Synth.* **2023**, https://doi.org/10.1038/s44160-023-00341-3.
[32] L. Liu, A. Corma, *Nat. Rev. Mater.* **2020**, *6*, 244.
[33] Q. Zhang, J. Guan, *Adv. Funct. Mater.* **2020**, *30*, 2000768.
[34] F. Maleki, G. Pacchioni, *ACS Catal.* **2021**, *11*, 554.
[35] E. W. McFarland, H. Metiu, *Chem. Rev.* **2013**, *113*, 4391.
[36] X. Li, H. Rong, J. Zhang, D. Wang, Y. Li, *Nano Res.* **2020**, *13*, 1842.
[37] C. Tang, L. Chen, H. Li, L. Li, Y. Jiao, Y. Zheng, H. Xu, K. Davey, S.-Z. Qiao, *J. Am. Chem. Soc.* **2021**, *143*, 7819.
[38] J. Cho, T. Lim, H. Kim, L. Meng, J. Kim, S. Lee, J. H. Lee, G. Y. Jung, K.-S. Lee, F. Viñes, F. Illas, K. S. Exner, S. H. Joo, C. H. Choi, *Nat. Commun.* **2023**, *14*, 3233.
[39] J. Zhang, H. Yang, B. Liu, *Adv. Energy Mater.* **2021**, *11*, 2002473.
[40] G. Di Liberto, L. A. Cipriano, G. Pacchioni, *ChemCatChem* **2022**, *14*, 202200611.
[41] J. K. Nørskov, T. Bligaard, A. Logadottir, J. R. Kitchin, J. G. Chen, S. Pandelov, U. Stimming, *J. Electrochem. Soc.* **2005**, *152*, J23.
[42] H. Xiang, W. Feng, Y. Chen, *Adv. Mater.* **2020**, *32*, 1905994.
[43] S. K. Kaiser, Z. Chen, D. Faust Akl, S. Mitchell, J. Pérez-Ramírez, *Chem. Rev.* **2020**, *120*, 11703.
[44] G. S. Parkinson, *Catal. Lett.* **2019**, *149*, 1137.
[45] F. Kraushofer, G. S. Parkinson, *Chem. Rev.* **2022**, *122*, 14911.
[46] H. V. Thang, S. Tosoni, L. Fang, P. Bruijnincx, G. Pacchioni, *ChemCatChem* **2018**, *10*, 2634.
[47] H. V. Thang, G. Pacchioni, L. DeRita, P. Christopher, *J. Catal.* **2018**, *367*, 104.
[48] H. V. Thang, G. Pacchioni, *J. Phys. Chem. C* **2019**, *123*, 7271.
[49] C. Asokan, H. V. Thang, G. Pacchioni, P. Christopher, *Catal. Sci. Technol.* **2020**, *10*, 1597.
[50] H. V. Thang, G. Pacchioni, *ChemCatChem* **2020**, *12*, 2595.
[51] H. V. Thang, F. Maleki, S. Tosoni, G. Pacchioni, *Top. Catal.* **2022**, *65*, 1573.
[52] S. Tosoni, G. Pacchioni, *Surf. Sci.* **2017**, *664*, 87.
[53] J. E. Bercaw, *Proc. Natl. Acad. Sci. USA* **2018**, *115*, 5049.
[54] X. Li, X. Yang, J. Zhang, Y. Huang, B. Liu, *ACS Catal.* **2019**, *9*, 2521.
[55] Y. Tang, C. Asokan, M. Xu, G. W. Graham, X. Pan, P. Christopher, J. Li, P. Sautet, *Nat. Commun.* **2019**, *10*, 4488.
[56] L. DeRita, J. Resasco, S. Dai, A. Boubnov, H. V. Thang, A. S. Hoffman, I. Ro, G. W. Graham, S. R. Bare, G. Pacchioni, X. Pan, P. Christopher, *Nat. Mater.* **2019**, *18*, 746.
[57] C. Paolucci, I. Khurana, A. A. Parekh, S. Li, A. J. Shih, H. Li, J. R. Di Iorio, J. D. Albarracin-Caballero, A. Yezerets, J. T. Miller, W. N. Delgass, F. H. Ribeiro, W. F. Schneider, R. Gounder, *Science* **2017**, *357*, 898.
[58] K. Reuter, M. Scheffler, *Phys. Rev. Lett.* **2003**, *90*, 46103.
[59] J. Yang, W. Liu, M. Xu, X. Liu, H. Qi, L. Zhang, X. Yang, S. Niu, D. Zhou, Y. Liu, Y. Su, J.-F. Li, Z.-Q. Tian, W. Zhou, A. Wang, T. Zhang, *J. Am. Chem. Soc.* **2021**, *143*, 14530.
[60] P. Poths, A. N. Alexandrova, *J. Phys. Chem. Lett.* **2022**, *13*, 4321.
[61] B. G. Levi, *Phys. Today* **1998**, *51*, 20.
[62] G. Di Liberto, S. Tosoni, L. A. Cipriano, G. Pacchioni, *Acc. Mater. Res.* **2022**, *3*, 986.
[63] L. Li, X. Chang, X. Lin, Z.-J. Zhao, J. Gong, *Chem. Soc. Rev.* **2020**, *49*, 8156.
[64] W. Zhang, Q. Fu, Q. Luo, L. Sheng, J. Yang, *JACS Au* **2021**, *1*, 2130.
[65] C. Mottet, J. Goniakowski, F. Baletto, R. Ferrando, G. Treglia, *Phase Transitions* **2004**, *77*, 101.
[66] A. Ruiz Puigdollers, P. Schlexer, S. Tosoni, G. Pacchioni, *ACS Catal.* **2017**, *7*, 6493.
[67] *Defects at Oxide Surfaces* (Eds: J. Jupille, G. Thornton), Springer International Publishing, Cham, Switzerland **2015**.
[68] K. Burke, L. O. Wagner, *Int. J. Quantum Chem.* **2013**, *113*, 96.
[69] J. P. Perdew, K. Burke, M. Ernzerhof, *Phys. Rev. Lett.* **1996**, *77*, 3865.
[70] J. P. Perdew, Y. Wang, *Phys. Rev. B* **1992**, *45*, 13244.
[71] A. D. Becke, *Phys. Rev. A* **1988**, *38*, 3098.
[72] C. Lee, W. Yang, R. G. Parr, *Phys. Rev. B* **1988**, *37*, 785.
[73] A. D. Becke, *J. Chem. Phys.* **1993**, *98*, 1372.
[74] A. D. Becke, *J. Chem. Phys.* **1993**, *98*, 5648.
[75] C. Adamo, V. Barone, *J. Chem. Phys.* **1999**, *110*, 6158.
[76] J. P. Perdew, M. Ernzerhof, K. Burke, *J. Chem. Phys.* **1996**, *105*, 9982.
[77] J. Heyd, G. E. Scuseria, M. Ernzerhof, *J. Chem. Phys.* **2003**, *118*, 8207.
[78] H. J. Kulik, M. Cococcioni, D. A. Scherlis, N. Marzari, *Phys. Rev. Lett.* **2006**, *97*, 103001.
[79] T. J. Goncalves, P. N. Plessow, F. Studt, *ChemCatChem* **2019**, *11*, 4368.
[80] C. A. Gaggioli, S. J. Stoneburner, C. J. Cramer, L. Gagliardi, *ACS Catal.* **2019**, *9*, 8481.
[81] A. Mitra, M. R. Hermes, M. Cho, V. Agarawal, L. Gagliardi, *J. Phys. Chem. Lett.* **2022**, *13*, 7483.
[82] J. Čížek, Adv. Chem. Phys. **1969**, *14*, 35.
[83] J. Čížek, *J. Chem. Phys.* **1966**, *45*, 4256.
[84] A. M. Patel, S. Ringe, S. Siahrostami, M. Bajdich, J. K. Nørskov, A. R. Kulkarni, *J. Phys. Chem. C* **2018**, *122*, 29307.
[85] I. Barlocco, L. A. Cipriano, G. Di Liberto, G. Pacchioni, *Adv. Theory Simul.* **2022**, https://doi.org/10.1002/adts.202200513.
[86] G. Di Liberto, L. A. Cipriano, G. Pacchioni, *ACS Catal.* **2022**, *12*, 5846.
[87] J. K. Nørskov, J. Rossmeisl, A. Logadottir, L. Lindqvist, J. R. Kitchin, T. Bligaard, H. Jónsson, *J. Phys. Chem. B* **2004**, *108*, 17886.
[88] S. Tosoni, G. Di Liberto, I. Matanovic, G. Pacchioni, *J. Power Sources* **2023**, *556*, 232492.
[89] T. Bligaard, J. K. Nørskov, S. Dahl, J. Matthiesen, C. H. Christensen, J. Sehested, *J. Catal.* **2004**, *224*, 206.
[90] J. K. Nørskov, T. Bligaard, A. Logadottir, S. Bahn, L. B. Hansen, M. Bollinger, H. Bengaard, B. Hammer, Z. Sljivancanin, M. Mavrikakis, Y. Xu, S. Dahl, C. J. H. Jacobsen, *J. Catal.* **2002**, *209*, 275.
[91] V. Pallassana, M. Neurock, *J. Catal.* **2000**, *191*, 301.
[92] G. Henkelman, B. P. Uberuaga, H. Jónsson, *J. Chem. Phys.* **2000**, *113*, 9901.
[93] E. Grifoni, G. Piccini, M. Parrinello, *J. Chem. Theory Comput.* **2020**, *16*, 6027.
[94] F. Fasulo, G. Piccini, A. B. Muñoz-García, M. Pavone, M. Parrinello, *J. Phys. Chem. C* **2022**, *126*, 15752.
[95] C. F. Dickens, C. Kirk, J. K. Nørskov, *J. Phys. Chem. C* **2019**, *123*, 18960.
[96] C. V. Ovesen, B. S. Clausen, B. S. Hammershøi, G. Steffensen, T. Askgaard, I. Chorkendorff, J. K. Nørskov, P. B. Rasmussen, P. Stoltze, P. Taylor, *J. Catal.* **1996**, *158*, 170.
[97] M. Pineda, M. Stamatakis, *J. Chem. Phys.* **2022**, *156*, 120902.
[98] C. T. Campbell, J. R. V. Sellers, *J. Am. Chem. Soc.* **2012**, *134*, 18109.
[99] A. Gross, M. Scheffler, *J. Vac. Sci. Technol., A* **1997**, *15*, 1624.
[100] G. Bertaina, G. Di Liberto, M. Ceotto, *J. Chem. Phys.* **2019**, *151*, 114307.
[101] F. Gabas, G. Di Liberto, M. Ceotto, *J. Chem. Phys.* **2019**, *150*, 224107.
[102] G. Collinge, S. F. Yuk, M.-T. Nguyen, M.-S. Lee, V.-A. Glezakou, R. Rousseau, *ACS Catal.* **2020**, *10*, 9236.
[103] A. B. Anderson, *Electrochim. Acta* **2003**, *48*, 3743.
[104] A. B. Anderson, *J. Electroanal. Chem.* **2021**, *898*, 115623.
[105] S. N. Steinmann, C. Michel, *ACS Catal.* **2022**, *12*, 6294.
[106] J. Tomasi, B. Mennucci, R. Cammi, *Chem. Rev.* **2005**, *105*, 2999.
[107] Z. Guo, F. Ambrosio, W. Chen, P. Gono, A. Pasquarello, *Chem. Mater.* **2018**, *30*, 94.
[108] Z.-D. He, S. Hanselman, Y.-X. Chen, M. T. M. Koper, F. Calle-Vallejo, *J. Phys. Chem. Lett.* **2017**, *8*, 2243.
[109] R. F. de Morais, T. Kerber, F. Calle-Vallejo, P. Sautet, D. Loffreda, *Small* **2016**, *12*, 5312.
[110] A. Bouzid, A. Pasquarello, *J. Chem. Theory Comput.* **2017**, *13*, 1769.

[111] G. Di Liberto, G. Pacchioni, Y. Shao-Horn, L. Giordano, *J. Phys. Chem. C* **2023**, *127*, 10127.
[112] F. Maleki, G. Di Liberto, G. Pacchioni, *ACS Appl. Mater. Interfaces* **2023**, *15*, 11216.
[113] G. Di Liberto, F. Maleki, G. Pacchioni, *J. Phys. Chem. C* **2022**, *126*, 10216.
[114] L.-M. Liu, C. Zhang, G. Thornton, A. Michaelides, *Phys. Rev. B* **2010**, *82*, 161415.
[115] N. Sathishkumar, H.-T. Chen, *ACS Appl. Mater. Interfaces* **2023**, *15*, 15545.
[116] D. D. Hibbitts, B. T. Loveless, M. Neurock, E. Iglesia, *Angew. Chem., Int. Ed.* **2013**, *52*, 12273.
[117] F. Calle-Vallejo, R. F. de Morais, F. Illas, D. Loffreda, P. Sautet, *J. Phys. Chem. C* **2019**, *123*, 5578.
[118] E. Romeo, F. Illas, F. Calle-Vallejo, *J. Phys. Chem. C* **2023**, *127*, 10134.
[119] K. Liu, J. D. Cruzan, R. J. Saykally, *Science* **1996**, *271*, 929.
[120] G. Di Liberto, R. Conte, M. Ceotto, *J. Chem. Phys.* **2018**, *148*, 104302.
[121] G. Di Liberto, L. Giordano, *Electrochem. Sci. Adv.* **2023**, https://doi.org/10.1002/elsa.202100204.
[122] M. C. O. Monteiro, F. Dattila, B. Hagedoorn, R. García-Muelas, N. López, M. T. M. Koper, *Nat. Catal.* **2021**, *4*, 654.
[123] J. T. Bender, A. S. Petersen, F. C. Østergaard, M. A. Wood, S. M. J. Heffernan, D. J. Milliron, J. Rossmeisl, J. Resasco, *ACS Energy Lett.* **2023**, *8*, 657.
[124] T. Cheng, L. Wang, B. V. Merinov, W. A. Goddard, *J. Am. Chem. Soc.* **2018**, *140*, 7787.
[125] N. Abidi, K. R. G. Lim, Z. W. Seh, S. N. Steinmann, *WIREs Comput. Mol. Sci.* **2021**, *11*, 1499.
[126] J. Sun, Y.-H. Fang, Z.-P. Liu, *Phys. Chem. Chem. Phys.* **2014**, *16*, 13733.
[127] R. Shang, S. N. Steinmann, B.-Q. Xu, P. Sautet, *Catal. Sci. Technol.* **2020**, *10*, 1006.
[128] Y. Ji, Y. Li, H. Dong, L. Ding, Y. Li, *J. Mater. Chem. A* **2020**, *8*, 20402.
[129] T. Wu, M. M. Melander, K. Honkala, *ACS Catal.* **2022**, *12*, 2505.
[130] Y.-Q. Su, Y. Wang, J.-X. Liu, I. A. W. Filot, K. Alexopoulos, L. Zhang, V. Muravev, B. Zijlstra, D. G. Vlachos, E. J. M. Hensen, *ACS Catal.* **2019**, *9*, 3289.
[131] M. Stamatakis, D. G. Vlachos, *J. Chem. Phys.* **2011**, *134*, 214115.
[132] E. F. Holby, G. Wang, P. Zelenay, *ACS Catal.* **2020**, *10*, 14527.
[133] Z.-J. Zhao, S. Liu, S. Zha, D. Cheng, F. Studt, G. Henkelman, J. Gong, *Nat. Rev. Mater.* **2019**, *4*, 792.
[134] Y. Guo, G. Wang, S. Shen, G. Wei, G. Xia, J. Zhang, *Appl. Surf. Sci.* **2021**, *550*, 149283.
[135] Y. Ouyang, L. Shi, X. Bai, Q. Li, J. Wang, *Chem. Sci.* **2020**, *11*, 1807.
[136] M. T. Darby, M. Stamatakis, A. Michaelides, E. C. H. Sykes, *J. Phys. Chem. Lett.* **2018**, *9*, 5636.
[137] L. Li, K. Yuan, Y. Chen, *Acc. Mater. Res.* **2022**, *3*, 584.
[138] X. Bai, Z. Zhao, G. Lu, *J. Phys. Chem. Lett.* **2023**, *14*, 5172.
[139] R. Réocreux, M. Stamatakis, *Acc. Chem. Res.* **2022**, *55*, 87.
[140] R. T. Hannagan, G. Giannakakis, R. Réocreux, J. Schumann, J. Finzel, Y. Wang, A. Michaelides, P. Deshlahra, P. Christopher, M. Flytzani-Stephanopoulos, M. Stamatakis, E. C. H. Sykes, *Science* **2021**, *372*, 1444.
[141] Z. Yao, Y. Lum, A. Johnston, L. M. Mejia-Mendoza, X. Zhou, Y. Wen, A. Aspuru-Guzik, E. H. Sargent, Z. W. Seh, *Nat. Rev. Mater.* **2022**, *8*, 202.
[142] L. Wu, T. Guo, T. Li, *J. Mater. Chem. A* **2020**, *8*, 19290.
[143] M. Umer, S. Umer, M. Zafari, M. Ha, R. Anand, A. Hajibabaei, A. Abbas, G. Lee, K. S. Kim, *J. Mater. Chem. A* **2022**, *10*, 6679.
[144] V. Fung, G. Hu, Z. Wu, D. Jiang, *J. Phys. Chem. C* **2020**, *124*, 19571.
[145] H.-C. Huang, Y. Zhao, J. Wang, J. Li, J. Chen, Q. Fu, Y.-X. Bu, S.-B. Cheng, *J. Mater. Chem. A* **2020**, *8*, 9202.
[146] H. Xu, D. Cheng, D. Cao, X. C. Zeng, *Nat. Catal.* **2018**, *1*, 339.
[147] X. Guan, C. Zhao, X. Liu, S. Liu, W. Gao, Q. Jiang, *J. Phys. Chem. C* **2020**, *124*, 25898.
[148] Z. Xue, X. Zhang, J. Qin, R. Liu, *Nano Energy* **2021**, *80*, 105527.
[149] X. Cui, W. Li, P. Ryabchuk, K. Junge, M. Beller, *Nat. Catal.* **2018**, *1*, 385.
[150] K. Christmann, *Surf. Sci. Rep.* **1988**, *9*, 1.
[151] R. H. Crabtree, *Acc. Chem. Res.* **1990**, *23*, 95.
[152] D. M. Heinekey, A. Lledós, J. M. Lluch, *Chem. Soc. Rev.* **2004**, *33*, 175.
[153] G. J. Kubas, *Chem. Rev.* **2007**, *107*, 4152.
[154] G. J. Kubas, *Acc. Chem. Res.* **1988**, *21*, 120.
[155] G. Di Liberto, L. A. Cipriano, G. Pacchioni, *J. Am. Chem. Soc.* **2021**, *143*, 20431.
[156] C. Saetta, G. Di Liberto, G. Pacchioni, *Top. Catal.* **2023**, *66*, 1120.
[157] M. M. Montemore, M. A. van Spronsen, R. J. Madix, C. M. Friend, *Chem. Rev.* **2018**, *118*, 2816.
[158] M. K. Coggins, X. Sun, Y. Kwak, E. I. Solomon, E. Rybak-Akimova, J. A. Kovacs, *J. Am. Chem. Soc.* **2013**, *135*, 5631.
[159] L. Vaska, *Acc. Chem. Res.* **1976**, *9*, 175.
[160] R. Boča, *Coord. Chem. Rev.* **1983**, *50*, 1.
[161] G. Pacchioni, *J. Chem. Phys.* **2008**, *128*, 18250.
[162] E. Sargeant, F. Illas, P. Rodríguez, F. Calle-Vallejo, *J. Electroanal. Chem.* **2021**, *896*, 115178.
[163] S. Dahl, A. Logadottir, R. C. Egeberg, J. H. Larsen, I. Chorkendorff, E. Törnqvist, J. K. Nørskov, *Phys. Rev. Lett.* **1999**, *83*, 1814.
[164] A. D. Allen, C. V. Senoff, *Chem. Commun.* **1965**, 621.
[165] D. Sellmann, *Angew. Chem., Int. Ed.* **1974**, *13*, 639.
[166] L. S. Yamout, M. Ataya, F. Hasanayn, P. L. Holland, A. J. M. Miller, A. S. Goldman, *J. Am. Chem. Soc.* **2021**, *143*, 9744.
[167] H.-J. Freund, R. P. Messmer, *Surf. Sci.* **1986**, *172*, 1.
[168] H.-J. Freund, M. W. Roberts, *Surf. Sci. Rep.* **1996**, *25*, 225.
[169] U. Burghaus, *Prog. Surf. Sci.* **2014**, *89*, 161.
[170] F. Solymosi, *J. Mol. Catal.* **1991**, *65*, 337.
[171] D. H. Gibson, *Coord. Chem. Rev.* **1999**, *185*, 335.
[172] X. Yin, J. R. Moss, *Coord. Chem. Rev.* **1999**, *181*, 27.
[173] I. Castro-Rodriguez, H. Nakai, L. N. Zakharov, A. L. Rheingold, K. Meyer, *Science* **2004**, *305*, 1757.
[174] E. Skúlason, G. S. Karlberg, J. Rossmeisl, T. Bligaard, J. Greeley, H. Jónsson, J. K. Nørskov, *Phys. Chem. Chem. Phys.* **2007**, *9*, 3241.
[175] S. Trasatti, *J. Electroanal. Chem. Interfacial Electrochem.* **1972**, *39*, 163.
[176] K. S. Exner, *Int. J. Hydrogen Energy* **2020**, *45*, 27221.
[177] Q. Tang, D. Jiang, *ACS Catal.* **2016**, *6*, 4953.
[178] R. M. Kluge, R. W. Haid, I. E. L. Stephens, F. Calle-Vallejo, A. S. Bandarenka, *Phys. Chem. Chem. Phys.* **2021**, *23*, 10051.
[179] I. Matanovic, K. Leung, S. J. Percival, J. E. Park, P. Lu, P. Atanassov, S. S. Chou, *Appl. Mater. Today* **2020**, *21*, 100812.
[180] K. S. Exner, T. Lim, S. H. Joo, *Curr. Opin. Electrochem.* **2022**, *34*, 100979.
[181] I. Barlocco, G. Di Liberto, G. Pacchioni, *Energy Adv.* **2023**, *2*, 1022.
[182] Y. Wu, C. Li, W. Liu, H. Li, Y. Gong, L. Niu, X. Liu, C. Sun, S. Xu, *Nanoscale* **2019**, *11*, 5064.
[183] L. Zhong, S. Li, *ACS Catal.* **2020**, *10*, 4313.
[184] I. Barlocco, L. A. Cipriano, G. Di Liberto, G. Pacchioni, *J. Catal.* **2023**, *417*, 351.
[185] H.-C. Tsai, T. H. Yu, Y. Sha, B. V. Merinov, P.-W. Wu, S.-Y. Chen, W. A. Goddard, *J. Phys. Chem. C* **2014**, *118*, 26703.
[186] L. A. Cipriano, G. Di Liberto, G. Pacchioni, *ACS Catal.* **2022**, 11682.
[187] T. D. Rapson, C. M. Gregg, R. S. Allen, H. Ju, C. M. Doherty, X. Mulet, S. Giddey, C. C. Wood, *ChemSusChem* **2020**, *13*, 4856.
[188] S. Agarwal, R. Kumar, R. Arya, A. K. Singh, *J. Phys. Chem. C* **2021**, *125*, 12585.
[189] X. Li, Q. Zhou, S. Wang, Y. Li, Y. Liu, Q. Gao, Q. Wu, *J. Phys. Chem. C* **2021**, *125*, 11963.
[190] C. Choi, S. Back, N.-Y. Kim, J. Lim, Y.-H. Kim, Y. Jung, *ACS Catal.* **2018**, *8*, 7517.

[191] T. Dai, Z. Wang, X. Lang, Q. Jiang, *J. Mater. Chem. A* **2022**, *10*, 16900.
[192] Y. Zhang, N. Ma, Y. Wang, B. Liang, J. Fan, *Appl. Surf. Sci.* **2023**, *623*, 156827.
[193] M. Behrens, F. Studt, I. Kasatkin, S. Kühl, M. Hävecker, F. Abild-Pedersen, S. Zander, F. Girgsdies, P. Kurr, B.-L. Kniep, M. Tovar, R. W. Fischer, J. K. Nørskov, R. Schlögl, *Science* **2012**, *336*, 893.
[194] S. Liu, H. Bin Yang, S. Hung, J. Ding, W. Cai, L. Liu, J. Gao, X. Li, X. Ren, Z. Kuang, Y. Huang, T. Zhang, B. Liu, *Angew. Chem., Int. Ed.* **2020**, *59*, 798.
[195] M. Li, H. Wang, W. Luo, P. C. Sherrell, J. Chen, J. Yang, *Adv. Mater.* **2020**, *32*, 2001848.
[196] D. Misra, G. Di Liberto, G. Pacchioni, *J. Catal.* **2023**, *422*, 1.

**Giovanni Di Liberto** is an assistant professor at University of Milano-Bicocca. He received his Ph.D. in chemistry developing theoretical methods for complex systems. He is currently working on the simulation of inorganic materials for applications in energy and environment, with particular attention to problems of thermal, photo, and electrocatalysis. He has been a visiting scientist at University of Barcelona since 2019.

**Gianfranco Pacchioni** (Ph.D. from Freie Universität Berlin in 1984) is active in the field of modeling of heterogeneous catalysis and oxide materials. He worked at the IBM Almaden Research Center, the Technical University of Munich, and the Fritz-Haber Institute (Berlin). He is a full professor at the University of Milano-Bicocca where he has been the Vice Rector for Research (2013–2019) and the Director of the Department of Materials Science (2003–2009). He is a co-author of 550 papers and has given more than 500 invited talks.